1993-03

A comparison of trans-equatorial ionosphere propagation predictions from AMBCOM with measured data

McKinstry, John W.

Monterey, California. Naval Postgraduate School

Approved for public release; distribution is unlimited.

A COMPARISON OF TRANS-EQUATORIAL IONOSPHERE PROPAGATION PREDICTIONS FROM AMBCOM WITH MEASURED DATA

by

John W. McKinstry
Lieutenant, United States Navy
B.S., Furman University, 1984

Submitted in partial fulfillment
of the requirements for the degree of

MASTER OF SCIENCE IN ELECTRICAL ENGINEERING

from the

NAVAL POSTGRADUATE SCHOOL
March, 1993

sified

' Classificaticr cf this page

REPORT DOCUMENTATION PAGE

ort Security Classification: Unclassified		1b Restrictive Markings			
urity Classification Authority		3 Distribution/Availability of Report Approved for public release; distribution is unlimited.			
lassification/Downgrading Schedule					
orming Organization Report Number(s)		5 Monitoring Organization Report Number(s)			
ie of Performing Organization Postgraduate School	6b Office Symbol *(if applicable)*EC/AB	7a Name of Monitoring Organization Naval Postgraduate School			
ress *(city, state, and ZIP code)* :rey CA 93943-5000		7b Address *(city, state, and ZIP code)* Monterey CA 93943-5000			
ie of Funding/Sponsoring Organization	6b Office Symbol *(if applicable)*	9 Procurement Instrument Identification Number			
s *(city, state, and ZIP code)*		10 Source of Funding Numbers			
		Program Element No	Project No	Task No	Work Unit Accession No

: *(include security classification)*A COMPARISON OF TRANS-EQUATORIAL IONOSPHERE PROPAGATION PREDICTIONS FROM AMBCOM WITH JRED DATA

sonal Author(s) McKinstry, John W.

pe of Report r's Thesis	13b Time Covered From To	14 Date of Report *(year, month, day)* March 1993	15 Page Count 93

plementary Notation The views expressed in this thesis are those of the author and do not reflect the official policy or position : Department of Defense or the U.S. Government.

ati Codes			18 Subject Terms *(continue on reverse if necessary and identify by block number)*
	Group	Subgroup	transequatorial, ionosphere, AMBCOM, propagation modeling

.ract *(continue on reverse if necessary and identify by block number)*

This thesis examines radio propagation conditions over trans-equatorial (TE) paths. The study precedes Project PENEX, a :xperiment to measure and collect calibrated HF skywave signal strength data for polar, equatorial, and near-vertical ·nce propagation paths. PENEX will benchmark the absolute accuracy of the signal-to-noise models in the MEDUSA gation model now being developed by the Naval Command, Control and Ocean Surveillance Center.

Since only minimal information is available about TE paths, a comprehensive review of the published literature on TE iments was completed, with emphasis on TE paths between magnetic conjugate points. Data from such paths have revealed ·esence of unusual propagation modes which are not predicted by standard propagation programs such as PROPHET, IONCAP, MBCOM. The review of the literature revealed that Stanford Research Institute (SRI) published measured data on a TE path en the Pacific islands of Kauai and Rarotonga.

A comparison was made between the SRI data and predictions for the same path to assess the usefulness of current :tion programs for TE paths. The SRI AMBCOM program was used for this comparison. As expected, sizeable differences were between the predicted and measured results, especially during times when unusual propagation modes were present. This sts that prediction programs should be modified to include the observed TE modes.

ribution/Availability of Abstract :lassified/unlimited _ same as report _ DTIC users	21 Abstract Security Classification Unclassified	
me of Responsible Individual rd W. Adler	22b Telephone *(include Area Code)* (408) 656-2352	22c Office Symbol EC/AB

.M 1473,84 MAR 83 APR edition may be used until exhausted — security classification of this pag

All other editions are obsolete — Unclassified

ABSTRACT

This thesis examines radio propagation conditions over trans-equatorial (TE) paths. The study precedes Project PENEX, a field experiment to measure and collect calibrated HF skywave signal strength data for polar, equatorial, and near-vertical incidence propagation paths. PENEX will benchmark the absolute accuracy of the signal-to-noise models in the MEDUSA propagation model now being developed by the Naval Command, Control and Ocean Surveillance Center.

Since only minimal information is available about TE paths, a comprehensive review of the published literature on TE experiments was completed, with emphasis on TE paths between magnetic conjugate points. Data from such paths have revealed the presence of unusual propagation modes which are not predicted by standard propagation programs such as PROPHET, IONCAP, and AMBCOM. The review of the literature revealed that Stanford Research Institute (SRI) published measured data on a TE path between the Pacific islands of Kauai and Rarotonga.

A comparison was made between the SRI data and predictions for the same path to assess the usefulness of current prediction programs for TE paths. The SRI AMBCOM program was used for this comparison. As expected, sizeable differences were found between the predicted and measured results, especially during times when unusual propagation modes were present. This suggests that prediction programs should be modified to include the observed TE modes.

TABLE OF CONTENTS

LIST OF TABLES

LIST OF FIGURES

I. INTRODUCTION

A. GENERAL

Radio propagation aspects of trans-equatorial (TE) paths are examined in this thesis. This study precedes a series of actual propagation measurements under Project PENEX to be conducted in 1993-94 by the Naval Security Group Command, the Naval Command, Control, and Ocean Surveillance Center, and the Naval Postgraduate School.

Since very little information is available in textbooks and standard documents about HF TE propagation, a comprehensive review of the literature was completed. A bibliography of pertinent documents is provided at the end of the thesis. Information obtained from documents in the bibliography were of interest and value in identifying TE information and experiments.

A number of experiments have been conducted over trans-equatorial paths, and many of the researchers involved have reported unusual TE propagation conditions. These unusual conditions have included propagation of unusual modes, at unexpected frequencies and anomalously high signal amplitudes. One particular experiment was of special interest, since one of the paths involved will most likely be the TE path for the PENEX study. Stanford Research Institute (SRI) conducted a series of experiments on TE paths in the Pacific region during the nuclear test series of 1962. The path from Kauai in the Hawaiian Islands to Rarotonga in the Cook Islands was of special interest because the two islands are situated very nearly at magnetic conjugate locations. Sounder data from this path were published by SRI [Ref. 1].

A comparison was made between this sounder data and a standard propagation prediction program. While several prediction programs could have been used for this purpose (e.g., PROPHET, IONCAP and others), the SRI AMBCOM program was used in this study.

This thesis is divided into five chapters. The first chapter provides an overview of Project PENEX, and a brief description of the morphology of the TE ionosphere as it applies to the AMBCOM program. The second chapter will describe the AMBCOM algorithms. Chapter III will characterize the 1962 SRI measured data and the experimental setup. The fourth chapter will compare AMBCOM predictions with SRI's measured data. Conclusions and recommendations are in Chapter V. The interested researcher will find a bibliography of the equatorial ionosphere and TE propagation at the conclusion.

B. PROJECT PENEX

PENEX is an acronym for Polar, Equatorial, and NVIS (Near-Vertical Incidence Skywave) Experiments. The objective of the PENEX experimental program is to measure and collect calibrated HF skywave signal strength data for the purpose of benchmarking the absolute accuracy of the signal to noise (S/N) models in the MEDUSA propagation models, now being developed by the Naval Command, Control, and Ocean Surveillance Center. Based on ten years operational experience and numerous comparisons to experimental data, the radiowave propagation models in PROPHET and MEDUSA provide very accurate median predictions for mid-latitudes. The same propagation models perform only marginally in predicting short term signal variations. In fact none of the existing propagation codes in use do a good job.

PENEX researchers will target the propagation characteristics in auroral and polar cap regions, trans-equatorial (TE) regions, and the propagation mode known as Near-Vertical Incidence Skywave (NVIS). Project PENEX is a 2-year study (1993-1994) of HF propagation, unique in utilizing a wide-band spread spectrum matched filter technique. Employing direct-sequence spread spectrum modulation techniques, GPS location data, and a rubidium clock, researchers expect the data generated to be very highly correlated. The wideband signal (about 40 kHz) approach is attractive and offers the following features:

1. Absolute signal recognition in almost any kind of interference environment (spread spectrum processing gains > 800).

2. Sufficient time resolution (12.5 μs time delay resolution) to identify each mode of propagation and the power density in that mode.

3. Significantly reduced output power requirements (< 100W).

The TE portion of the experiments, the subject of the current thesis, is scheduled to be conducted in 1993-94 with a transmitter located on Kauai in the Hawaiian Islands and a receiver on Rarotonga in the Cook Islands.

C. THE TRANS-EQUATORIAL IONOSPHERE

1. Geomagnetic and Solar Parameters

a. The Geomagnetic Coordinate System

The Earth's magnetic field may be approximated by an earth-centered dipole directed southward and inclined at about 11.5° to the earth's rotational axis. Presently, the northern pole of the dipole is located approximately at 81° N, 84.7° W using the geographic coordinate system [Ref. 2: p.60]. When studying or modeling the ionosphere, the geomagnetic coordinate system is commonly used to map the ionosphere to an earth-bound coordinate system. The geomagnetic coordinate system is based upon the geographic location of the earth's magnetic poles. The longitudinal origin for this system is the meridian line which passes through the north and south geomagnetic poles and through the geographic south pole. The two systems are related with the equations [Ref. 3: p.40]

$$\sin \Phi = \sin\phi \sin\phi_0 + \cos\phi \cos\phi_0 \cos(\lambda - \lambda_0), \tag{1}$$

and

$$\sin \Lambda = \cos\phi \sin(\lambda - \lambda_0) / \cos \Phi, \tag{2}$$

where

ϕ_0 = geographical latitude for the northern geomagnetic pole,

λ_0 = geographical longitude for the northern geomagnetic pole,

ϕ = geographical latitude,

λ = geographical longitude,

Φ = geomagnetic latitude and

Λ = geomagnetic longitude.

Although the AMBCOM program makes the geographic-to-geomagnetic coordinate conversion for the user, an understanding of the geomagnetic coordinate system is useful in understanding the model.

b. Geomagnetic Activity Indices

AMBCOM uses the three-hour K_p index of worldwide magnetic disturbance to specify the current state of the earth's magnetic field. This index is based upon local K indices which are quasi-logarithmic values prepared at twelve selected observatories worldwide to describe the condition of the planetary magnetic field at each site. These local K values are corrected to calculate the planetary K_p index. The K_p index is calculated at three hour intervals for each of eight periods per day. The K_p indices range from zero, the least disturbed state, to nine which represents the most disturbed magnetic field. The K_p indices used for this thesis are published in the *Journal of Geophysical Research* [Refs. 4,5,6,7] and are listed in Appendix B. For this study the indices ranged from zero to seven, indicating that the geomagnetic field varied from a nondisturbed state to a considerably disturbed state.

c. Sunspot Number

Sunspots, related to the solar flux, are characterized by strong magnetic fields which may approach 0.4 Tesla. They have approximately an 11-year periodicity in occurrence. Their occurrence was measured by the Wolf, or Zurich sunspot number, R_z [Ref. 2: p.29],

$$R_z = k(10g + s) \quad (3)$$

where

g = number of sunspot groups observed,

s = number of observed individual spots and

k = correction factor.

Daily values of R_z used in the present study were also derived from the *Journal of Geophysical Research* [Refs. 4,5,6,7] and are listed in Appendix B. The R_z number was discontinued in 1981 in favor of the International Sunspot Number, R_I [Ref. 2: p. 44].

2. Ionospheric Layers

Radio waves may be refracted or reflected as they encounter ionospheric layers during propagation. As rays move through various areas of the atmosphere, gradual changes occur in the speed of the waves as the temperature, air density, and levels of ionization change. On frequencies below 30 MHz, long distance communication is the result of refraction of the wave in the ionosphere, where free ions and electrons exist in sufficient quantity to affect the velocity of wave travel. Depending on the frequency used and the time of day, the ionosphere can support communications from very short ranges of less than 100 km (Near Vertical Incidence Signals - NVIS) to distances greater than 9500 km.

Ionization of the upper atmosphere is attributed to ultraviolet radiation from the sun, and results in several layers of varying densities at various heights surrounding the Earth. Each layer has a central region of maximum electron density, which tapers off both above and below that altitude. The ionospheric layers that most influence HF communications are the D, E, E_s, F_1, and F_2 layers (Fig. 1). Of these, the D layer, with altitudes of 50-90 km, absorbs signals passing through it. The lowest region useful for returning radio signals to the Earth at HF is the E layer, with altitudes of 80-150 km. Its average height of maximum ionization is about 100 km. The layer refracts waves only in the presence of sunlight. Ionization is greatest around local noon, and practically disappears after sundown.

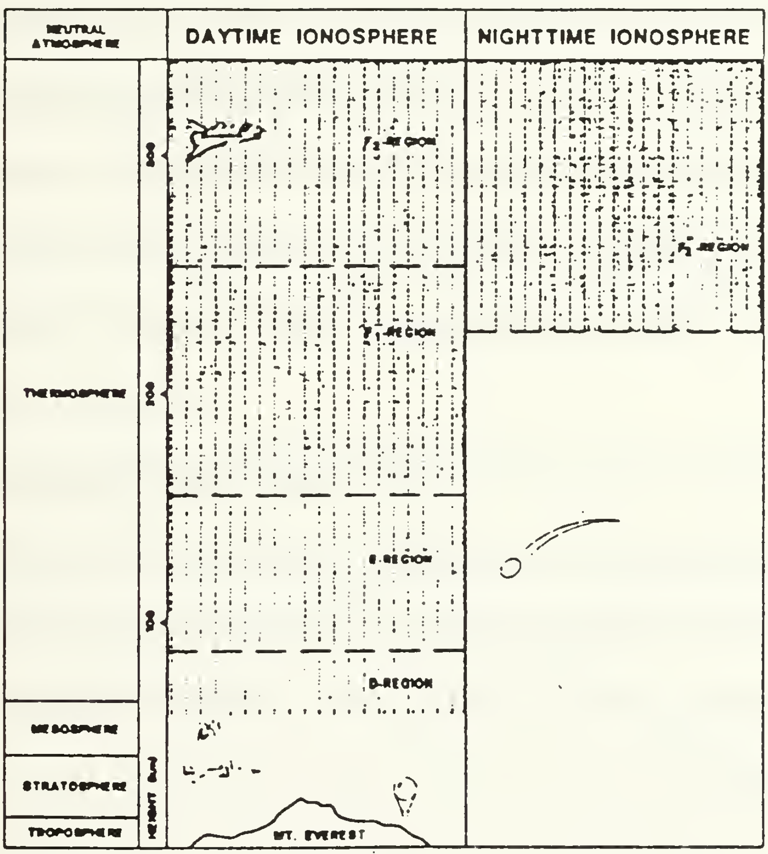

Figure 1. The Ionospheric Layers [From Ref. 8]

The sporadic-E region, E_s consists of relatively dense patches of ionization that drift around from 90-130 km above the Earth. Its effects become prominent above 21 MHz and into the VHF region.

The region of ionization mainly responsible for long distance communication is the F-layer. Its altitudes of ionization range from 150-600 km. It ionizes very rapidly at sunrise, reaching peak electron density early in the afternoon at the middle of the propagation path. The ionization decays very slowly after sunset, reaching the minimum value just before sunrise. During the day, the F region is split into two layers, the F_1 and the F_2. The F_1 layer is usually not an important propagation medium unless it supports the only mode to propagate. Its refracting heights are between 150-200 km, forming and fading with the passage of the sun. After sunset, the F_1 layer decays and is replaced by a broadened F_2 layer, the primary medium supporting HF communications. The thickness of the layer ranges from 80 km during the day to a broad 150 km about 320 km above the Earth at night. The maximum range of a single hop off the F_2 layer is about 4000 km. [Ref. 8]

Traditionally, the ionospheric layers have been characterized as well-behaved stratified layers. From very high resolution measurements of the medium, it is now widely accepted that the layers are in continual horizontal and vertical motion. Periods of high solar activity, with their impact on the ionosphere, often result in unusual propagation modes.

3. Sporadic E (E_s)

Sporadic E is a thin reflecting layer in the ionosphere which comes and goes sporadically at E-region heights. The most important aspect of E_s is the maximum electron density or critical frequency, f_oE_s, and its daily and seasonal variations. [Ref. 8: p.29]

Low-latitude or equatorial E_s is basically a daytime phenomenon with little seasonal variation. Near the geomagnetic equator the critical frequency f_oE_s exceeds 5 MHz for 90% of the daylight hours. Equatorial E_s is due to a plasma instability caused by the high electron drift velocity. It is patchy and transparent, but seems to be a useful reflector on long TE circuits, making it possible to get higher MUFs than would be expected for normal propagation [Ref. 8: p.125].

Variations of the ionosphere at low latitudes are so strongly influenced by the earth's magnetic field, that it is usually more instructive to consider how the ionosphere varies with geomagnetic latitude or with dip angle of the earth's magnetic field rather than within a geographic framework.

4. Trans-equatorial Propagation (TEP)

In low-latitude ionospheres, the "fountain effect" redistributes electrons, moving them from the equator north and south to magnetic latitudes of 10° to 20°. The electromagnetic field causes electrons to drift upwards, encountering the horizontal lines of force of the earth's magnetic field. Electrons diffuse down these field lines to reenter the main body of the ionosphere where the field lines cut through the F region. This causes large clumps of electrons at latitudes 10° to 20° from the magnetic equator. These clumps are the peaks or "crests" of the equatorial or Appleton anomaly.[Ref. 8: p.30]

These crests are most developed in the late afternoon and early evening, during the equinoxes, and at solar maximum. Their critical frequencies, f_oF_2, can exceed 20 MHz as compared to 10 MHz at the equator. The height of maximum electron density, h_mF_2, is less at the crests than at the equator. The significant change with latitude of f_0F_2 and h_mF_2 is difficult to predict and may be responsible for some of the interesting propagation modes observed in the TE environment. [Ref. 8: p.30]

Discovered in 1947 by radio amateurs, trans-equatorial (TE) propagation occurs on circuits which cross the equator, more or less at right angles, and have MUFs (maximum usable frequency) higher than the normal multihop modes. Stations attempting TE contacts must be nearly equidistant from the geomagnetic equator. Two types of TE propagation depend on different features of the equatorial ionosphere for their characterization [Refs. 9,10,11,12]. These are afternoon-type TE propagation (A-TEP) and evening-type TE propagation (E-TEP). Both types have been observed simultaneously on some circuits around 2000 local time [Ref. 8: p.126].

a. *Afternoon-type TEP*

A-TEP has the following characteristics:

- MUF greater than the normal 2F MUF, i.e., greater than 40-50 MHz.
- peak occurrence from 1700-1900 local time, near the equinoxes and at solar maximum.
- path lengths of greater than 6000 km.

- strong steady signals with low fading rates and small doppler spread

Several theoretical models have been proposed in the past to describe the propagation mechanism in TEP circuits. Initially a double refraction scheme from the ionospheric crests was proposed [Ref. 13]. Although this model explains quite satisfactorily the A-TEP phenomena, it fails to predict the E-TEP basic characteristics [Refs. 9, 14].

Raytracing algorithms [Ref. 15] have determined the propagation mode for these signals is a "super mode" or FF mode, where the signal is reflected twice by the F layer, on opposite sides of the equator, without a ground reflection. Figure 2 illustrates this super mode, which is dependent upon the electron density concentrations in the anomaly crests already discussed. The crests occur at about 15° dip angle north and south of the magnetic equator where h_mF_2 is at a minimum. Therefore, a ray leaving a suitably placed transmitter can be reflected from the first crest in a direction to miss the Earth and

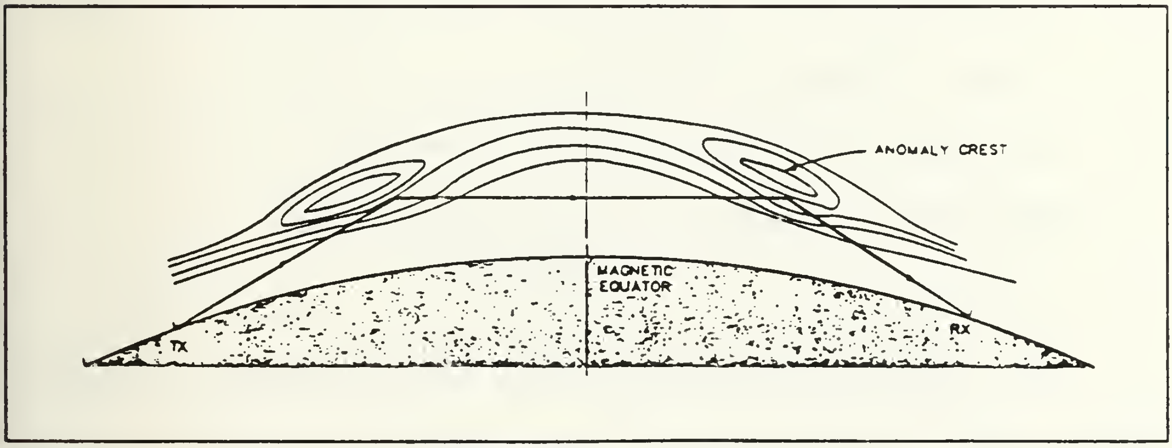

Figure 2. The "Super-Mode" or FF mode responsible for A-TEP [From Ref. 8]

strike the ionosphere at the opposite crest, before reflection back to the receiver. The MUF would be higher than the normal 2F MUF since the ionosphere at the crests is tilted upwards towards the magnetic equator, giving rise to larger angles of incidence. The MUFs are also higher because the critical frequencies are so high in the crests.

Maximum observed frequencies (MOF) for this super mode can exceed 50 MHz. The high signal strengths are the result of focussing effects as rays arrive from a large range of elevation angles. Signals also pass through the absorbing D region only twice, as opposed to four times for a 2F mode, and are, therefore, less attenuated. This supermode occurs most frequently during equinoxes at solar maximum, and then not every day. Its occurrence depends on how the crests developed for a specific day.

b. Evening-type TEP

E-TEP usually supports higher frequencies than A-TEP and has different characteristics:

- peak occurrence from 2000-2300 local time, near equinoxes and near solar maximum.
- high signal strengths but with deep and rapid fading, and a large doppler spread, which can exceed 40 Hz.
- path lengths shorter than A-TEP, about 3000-6000 km.
- higher MOFs than A-TEP, can be greater than 100 MHz.

Based on measurements of elevation angles and group delays on a circuit between Japan and Australia a waveguide model has been suggested for the E-TEP [Ref.

16]. The guiding of high frequency waves through field aligned irregularities has been examined theoretically by Nielson [Ref. 17], and this theory has been extended by using numerical techniques to explain TEP phenomena by Heron and others [Ref. 18]. A "whispering gallery" mode has also been considered to describe TEP [Ref. 19]. Data gathered for the fine structure of ionosphere has shown that there are elongated irregularities aligned with the geomagnetic field lines in the equatorial ionosphere [Ref. 20]. These are tubular shape depletion regions inside the equatorial ionosphere extending on both sides of the magnetic equator at least from 5° to 10° (magnetic dip). [Ref. 14]

The propagation mode for E-TEP is probably the "whispering gallery" or "field-guided" mode. Range spreading on evening ionograms indicate that the equatorial ionosphere is threaded with "empty" tubes aligned along magnetic field lines where the electron density is much lower than that of the surrounding ionosphere. Figure 3 shows that the propagation takes place by rays skidding around the walls of the tube, bouncing off the walls, and emerging at the far end of the tube [Ref. 21].

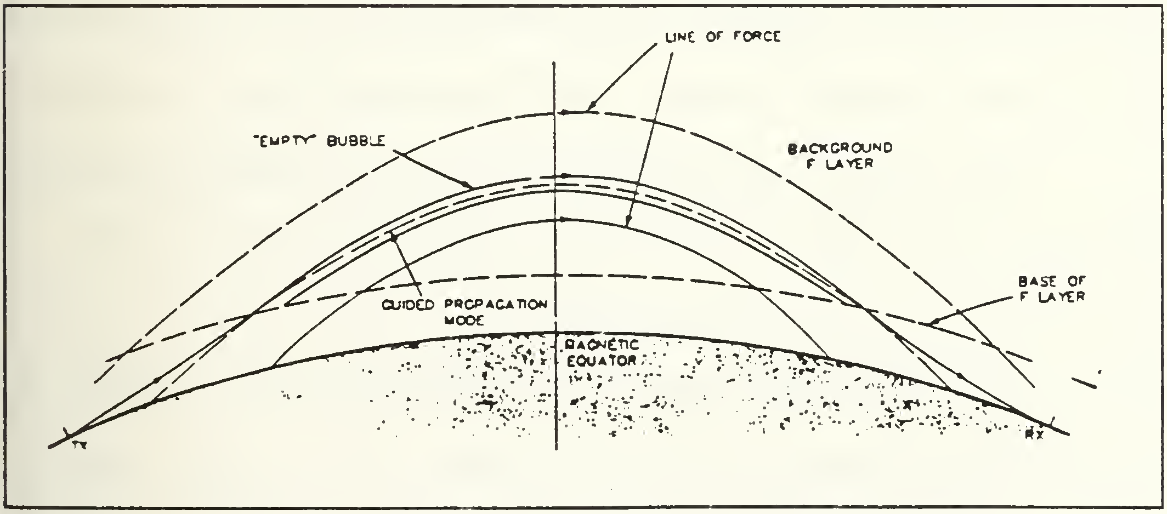

Figure 3. The Field-guided mode responsible for E-TEP[From Ref. 8]

MOFs have been noted over 100 MHz, arising from very high angles of incidence. Large doppler shifts would be caused by the upward movement of the tubes, which rise rapidly to the top of the ionosphere after their creation near the base. The best circuits to support this theory place the transmitter tangential to the earth's magnetic field so rays commence at the altitude to enter the tubes. Highest MUFs would be achieved when the receiver is similarly placed. The circuit, therefore, should be symmetric about the magnetic equator, with transmitter and receiver located at magnetic conjugate points, as is the case with the Kauai-Rarotonga path. Like A-TEP, E-TEP is unpredictable night to night.

II. THE AMBIENT COMMUNICATIONS MODEL (AMBCOM)

A. INTRODUCTION

This chapter provides a brief description of applicable portions of the AMBCOM program. Details of the complete program and code are contained in the user's guides published by SRI International [Refs. 22,23,24].

AMBCOM was designed for batch processing using card images as input. Separate programs support each of the function areas modelled, i.e., the ionosphere model is generated by a program which passes its data to another program for calculating raytracing curves. The system flow is first explained followed by the programs and inputs which generated the TE data for the Kauai-Rarotonga path.

B. SYSTEM FLOW

The AMBCOM system is a multiprogram batch system written in FORTRAN and was executed on a VAX 3100 workstation at NPS. Programs NATGEN, RAYTRA, and COMEFF were used to generate the TE data, as shown in Figure 4. Data are passed between these programs by means of saved data files [Ref. 22: pp.107-155].

The execution input streams were constructed for each of the 123 days in the period of interest, July-October 1962. A file of 57 lines of code comprising the input streams for NATGEN, RAYTRA and COMEFF was executed successively for each day. In order to obtain a complete 24-hour table of the spectrum of interest, each day's input file

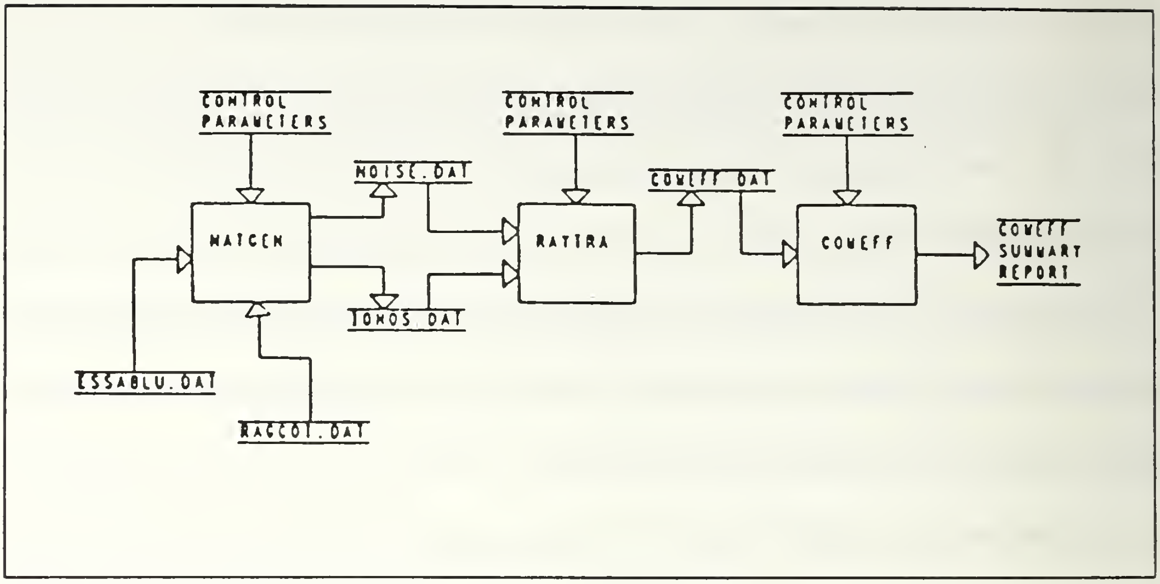

Figure 4. AMBCOM System Flow [From Ref. 25]

included as a parameter the average of the eight daily K_p indices (App. B). Total execution time for the 123 day campaign was three and half hours.

C. NATGEN

1. Overview

The purpose of NATGEN is to model the ionosphere along the communications path between two points. NATGEN builds a model of the F_2, F_1, and E layers at control points along the path. The control points are evenly spaced at 100 km increments with a maximum of 41 control points for paths longer than 4000 km. The control points are not necessarily located at the signal reflection points since raytracing is performed in RAYTRA. [Ref.22: pp.23-24]

NATGEN begins by reading ionospheric coefficients provided by the Institute for Telecommunications Sciences (ITS) in Boulder, Colorado, based upon the month, day, and the current sunspot number (input stream variables). AMBCOM uses the ITS Blue Deck (a reference to earlier coefficient files that were issued on color coded computer cards) as the starting point for modeling the F_2, F_1, and E layers at each control point. Additional parameters describing atmospheric noise, ground conductivity, and ground permittivity along the path are read and passed to RAYTRA. [Ref. 22: p.23]

The semithicknesses, heights of maximum ionization, and the critical frequencies for the F_2, F_1, and E layers at each of the control points are passed as outputs from NATGEN. ITS upper, median, and lower decile values for sporadic E critical frequencies are passed to RAYTRA which performs all E_s calculations. NATGEN also passes on the location of the transmitter and receiver sites, the time of year, time of day, the current K_p index, the sunspot number, distance between control points, the number of control points, and the path length. [Ref.23: pp.123-124]

2. Layer modeling

The ITS ionosphere provides the vertical incident critical frequency (f_o) for the E layer, the F_2 layer, and sporadic E. The E layer critical frequency (f_oE) is always set to the median decile values. For the sporadic E and the F_2 layers, the upper, median, and lower decile values represent the critical frequencies 90%, 50%, and 10%, respectively, of the days for a given time and month [Ref. 26: p.89]. NATGEN allows the user to choose which of the F_2 layer values will be used as the F_2 critical frequency (f_oF_2) for all ionospheric calculations. The default f_oF_2 value is the median decile number, and was used in this study. Two additional parameters for the F_2 layer are the ratio of the semithickness of the layer (y_m) to the height of maximum density (h_m) and the maximum usable frequency (MUF) for a 3000 km path (M3000). [Ref. 22: p.25]

Using these coefficients, AMBCOM models the ionosphere at the control points. The F_2, F_1 and E layers are represented as three parabolic layers with the values for the F_1 layer derived from the F_2 and E layer models. The height and semithickness of the E layer are set at 115 km and 25 km respectively. The F_2 layer height is calculated using the ITS coefficients in a two step process. First the peak height of the F_2 layer (HP_{F2}) is calculated using the Shimazaki equation [Ref. 22: p.26]

$$HP_{F2}= (1490/M3000) -176 \tag{4}$$

This value is corrected for signal retardation with a height factor (Δh) equation [Ref. 22: p.26]

$$\Delta h = [f/f_c \ln\{(f/f_c+1)/(f/f_c-1)\} -2]y_m \tag{5}$$

where

Δh = the height error,

f_c = the critical frequency of the layer,

f = the transmitted frequency and

y_m = the semithickness of the layer.

The Δh factor is then subtracted from HP_{F2} to produce a corrected height for the F_2 layer.

The F_1 layer parameters are not represented by ITS data but are calculated using the E and F_2 layer parameters. The F_1 layer must overlap the F_2 layer by half of its own semithickness with the bottom of the F_1 layer set at 130 km. The critical frequency of the F_1 layer is calculated based upon the critical frequency of the E layer

(f_0E). In the event that the F_2 layer critical frequency is lower than that for F_1, f_0F_1 is set to 0.695. [Ref. 22: p. 27]

3. NATGEN Input Variables

AMBCOM is a batch system in which an input stream controls the execution of the system and resembles a series of 80 column computer cards. AMBCOM was originally designed during the 1970s when card input systems still predominated [Ref. 22: p.15). Figure 5 is an example of statements used to execute NATGEN. The ASSIGN statements provide NATGEN access to the ITS file (ESSABLU.DAT), the conversion tables for the geomagnetic coordinate system (RAGCOT.DAT), two output files (IONOS.DAT and NOISE.DAT), and execution control cards one through four.

AMBCOM provides a large amount of flexibility in the control of data production. NATGEN models the ionosphere along any propagation path at any hourly time increment specified by the numbered control cards. The AMBCOM user defines the problem by specifying the transmitter and receiver locations, the sunspot number, the K_p index, and the time increment.

Control parameters were chosen to model the ionosphere, as closely as possible, to the 1962 SRI transmission paths. The intent was to execute the model from the perspective of a communicator who is attempting to estimate the possibility of communicating with another HF site under a given set of circumstances. Although the communicator does not have the advantage of using the sunspot number and K_p index

```
$1345678901234567890123456789012345678901234567890123456789012345678901234567890
$!
$! *** OCTOBER 1962 ***
$! FREQUENCY MANAGEMENT BETWEEN A SPECIFIED TRANSMITTER AND RECEIVER
$! *** INPUT SETUP FOR NATGEN ***
$SET DEF DKA0:[AMBCOM]
$ASSIGN DKA0:[AMBCOM]ESSABLU.DAT FOR001:
$ASSIGN DKA0:[AMBCOM]RAGCOT.DAT FOR075:
$ASSIGN DKA0:[AMBCOM]IONOS.DAT FOR002:
$ASSIGN DKA0:[AMBCOM]NOISE.DAT FOR004:
$ASSIGN SYS$INPUT FOR058:
$ASSIGN DKA0:[MCKINSTRY]NATOUT.DAT FOR059:
$R DKA0:[AMBCOM]NATGEN
1        0        0        0        0        0        0
 BEGIN THESIS WORK WITH AMBCOM
2        1                                            1
3     22.00   -159.50    -21.20   -159.80     1962     10.0      43.0      4.4
4       0.0      22.0       2.0
```

Figure 5. NATGEN control cards used to model Kauai-Rarotonga path

tables for a current month, he should have a rough estimate of the current sunspot number and K indices at any given time.

Figure 5 shows the four control cards used to execute NATGEN. Card one is used to edit ionospheric parameters, and card two causes NATGEN to run the ionospheric generator program. Card three defines the geographic latitude and longitude of the transmitter and receiver; negative numbers indicate a west longitude or south latitude. Following the location information are the year, month, sunspot number, and K_p index. Card four indicates the beginning hour, ending hour and time increment.

Input streams were divided into one-day periods for the four-month study, with each day represented by an average K_p index. The values for sunspot number and K_p index were taken from the *Journal of Geophysical Research* [Refs. 4,5,6,7].

D. RAYTRA

1. Overview

The raytracing program (RAYTRA) model can be executed in two modes, point-to-point and radar. The point-to-point mode, used in this thesis, performs raytracing from a transmitter to a receiver. RAYTRA computes group times, phase times, signal losses, the effects of sporadic E and elevation angles at both sites. These data are saved for each successful propagation path and are passed to COMEFF.

The raytracing algorithm computes the propagation path based on data produced by NATGEN. A raytrace which ends within 1000 km of the receiver site is saved for further processing. When two rays bracket the receiver, the program interpolates a ray that falls within some preset value, in this case ten kilometers. The parameters describing this ray are saved for COMEFF. In the case where only a single ray is found, the program again interpolates until a ray close to the receiver is found. The AMBCOM User's Guide for Engineers [Ref.22: pp.35-56] provides an in-depth treatment of raytrace algorithms.

RAYTRA estimates the amount of absorption for each ray. The absorption calculations are divided into four parameters as follows:

- L_D is the divergence, i.e., free space spreading loss.
- L_A is ionospheric absorption loss such as deviative, nondeviative, and auroral losses.
- L_{Es} is the loss resulting from sporadic E.
- L_G is the loss due to ground reflection along the path.

The total loss for a path is the summation of all of these factors. A full explanation of the RAYTRA path loss algorithms may be found in [Ref. 22: pp.56-80].

2. Sporadic E Calculations

RAYTRA offers two choices for computing sporadic E (E_s). The first method computes the reflection of a signal for frequencies below the blanketing frequency (f_bE_s). The blanketing frequency is computed based upon the location of the control point. The second method performs E_s reflection calculations for all frequencies less than f_oE_s. The value for f_oE_s is based upon the upper, median, or lower ITS f_oE_s coefficients passed from NATGEN. The choice of value is specified by the user. RAYTRA calculates f_oE_s dependent upon the percentage of E_s specified by the user. If 90% E_s is specified then RAYTRA uses the upper decile value of f_oE_s from the ITS file. For 50% E_s RAYTRA used the median decile value.

3. RAYTRA Input Variables

RAYTRA, like NATGEN, provides the user with a number of options for controlling program execution. Options are specified with numbered control cards which represent input streams following the program execution statement. Figure 6 is an example of the RAYTRA controlling statements used for this thesis.

Card two controls the amount of E_s for a given execution. For this study, the default value of 50% was used. Card two also allow the user to set the level of man-made noise at the receiver. A residential or suburban setting was assumed as a liberal

```
$1345678901234567890123456789012345678901234567890123456789012345678901234567890
$!   ***INPUT SETUP FOR RAYTRA ***
$SET DEF DKA0:[AMBCOM]
$ASSIGN SYS$INPUT FOR060:
$ASSIGN DKA0:[MCKINSTRY]RAYOUT.DAT FOR059:
$ASSIGN DKA0:[AMBCOM]COMEFF.DAT FOR007:
$R DKA0:[AMBCOM]RAYTRA
1                  0                                 0          0           0           0
2      22.00   -159.50     -21.20    -159.80          0.0        -2.          0.0         0.0
3        4.0       2.0       40.0        2.0          2.0       60.0        . .6          .6
5          1         0          4
8          0         0          0          0            0          0           0
0
0
0
0
0
0
0
0
0
0
0
0
1          0         1
```

Figure 6. RAYTRA input stream used to model Kauai-Rarotonga path

estimate of the noise environment.

Frequencies for RAYTRA are specified by control card three. Frequencies from 4-64 Mhz were initially executed to model as closely as possible the SRI experiment. Unfortunately, the antenna configuration pattern in AMBCOM only allows frequencies of 3-33 Mhz to be transmitted, so the 4-64 Mhz input range always failed to show propagation above about 40 Mhz. For the remainder of the study, RAYTRA input was set to 4-40 Mhz, with successful propagation up to about 30-32 MHz.

E. COMEFF

1. Overview

The communications effect (COMEFF) program evaluates the quality of a transmitted signal. NATGEN and RAYTRA dealt with the ionosphere and possible ionospheric effects along a given propagation path. The only site-dependent information for those two programs were the site locations. COMEFF parameters include transmit power, antenna configuration, signal bandwidth, and other communication site-dependent data. Based upon these local parameters and the data produced by RAYTRA, the performance of a particular communications link using a given frequency can be characterized in terms of the signal-to-noise ratio (SNR), field strengths and doppler spread.

2. Program Features

COMEFF uses the data generated by RAYTRA for all of the saved modes as the basis for evaluation of a particular communications link. The raytrace descriptive data, for each ray, includes:

- take-off angle,
- group time,
- phase time,
- path loss,
- noise power (per 1 Hz),
- arrival angle and
- transmitter frequency [Ref. 22: p.112].

Multiple raytraces may be described for each frequency. COMEFF combines the effects of multiple modes to produce a single reception statistic.

COMEFF allows the user to include the effects of the antenna configuration on the communications link. The antenna data is taken from ANTLIB.DAT, the

AMBCOM antenna file. ANT726 was used as a Granger Associates vertically polarized log-periodic antenna [Ref. 27]. Appendix A contains the antenna gain table for the ANT726 antenna used at both transmitter and receiver in this thesis.

The COMEFF program provides a variety of output options. COMEFF will calculate the SNR, group time, doppler shift, phase, and delay spread for all frequencies specified in RAYTRA. Other options provide field strengths or analysis of signal quality as bit error rate. All requested data may be printed in several formats which include a listing of SNR, doppler shift, phase shift, and group times for each mode. COMEFF also produces a single report that sums the data for each frequency at a particular time. The SNR specified in the COMEFF summary report is a weighted accumulation of SNRs for all modes received from RAYTRA.

Weighted SNRs from the COMEFF summary report were compared to SRI's propagation spectrum, which lacked specific SNR data. This composite SNR is calculated by computing the power for each ray, combining these values and then subtracting the noise value. The power A_i for each ray is computed with the equation

$$A_i = (P_t G_t G_r c^2)/4\pi L_i f^2 10^{12} L_r \qquad (6)$$

where

P_t = transmitter power (W),

G_t = transmitter antenna gain,

G_r = receiver antenna gain,

L_i = path loss for the ith ray,

L_r = receiving antenna loss,

c = speed of light and

f = frequency (MHz).

The composite SNR value is given by the equation

$$\mathrm{SNR} = 10 \log_{10}(\Sigma A_J) - N_e, \tag{7}$$

where N_e is the noise power density in dBW. [Ref. 22: p.83]

3. COMEFF Input Variables

Figure 7 is an example of the COMEFF input stream. Two control cards control program execution. The first card specifies transmit power, and path loss threshold. A bandwidth of 4 kHz and a transmitter power of 30 kW for SRI's sounder transmissions results in 7.5 W/Hz. The path loss threshold excludes modes with a path loss greater than the specified threshold. This parameter was set at 300 dB which effectively allowed all modes to be included. The second COMEFF control statement specifies antennas.

```
$!   ***INPUT SETUP FOR COMEFF
$!34567890123456789012345678901234567890123456789012345678901234567890
$SET DEF DKA0:[AMBCOM]
$ASSIGN SYS$INPUT FOR055:
$ASSIGN DKA0:[MCKINSTRY]WAVFORM.DAT FOR020:
$ASSIGN DKA0:[MCKINSTRY]COMOUT.DAT FOR059:
$ASSIGN DKA0:[AMBCOM]ANTLIB.DAT FOR006:
$R DKA0:[AMBCOM]COMEFF
 KAUAI-RAROTONGA PATH 25 OCTOBER 1962
    0   1. 2200   0    1    0         7.5        0.  300    1    0    0        1.0
ANT726      ANT726                                1
$SET DEF [MCKINSTRY]
$EXIT
```

Figure 7. COMEFF control input used to model Kauai-Rarotonga path

III. THE SRI TRANS-EQUATORIAL EXPERIMENTS

A. GENERAL

From June through October 1962, Stanford Research Institute (SRI) operated oblique incidence sounders on a 4800-km TE path from Kauai to Rarotonga as part of the test instrumentation for the 1962 nuclear tests in the Pacific. Workers observed anomalous propagation of HF modes from low HF into the VHF range across the TE path, and noticed this as a nocturnal phenomenon, occurring between sunset and sunrise. The propagation was unusual in that frequencies much higher than would usually be predicted were propagated over very long distances. This occurred on over 80% of summer nights and nearly 100% of nights during the equinoctial months. It was also observed that the mode showed a slight inverse correlation with magnetic activity, appearing later on magnetically disturbed days. The mechanism involved was believed to depend on field-aligned ionization and dip angle as it relates to the magnetic field symmetry. [Ref. 1]

B. THE EXPERIMENT

The observations made by SRI resulted as an outgrowth of the 1962 Pacific nuclear test series. Specific paths and equipment used were not selected specifically for the study of TE propagation.

One path studied was from Kauai in the Hawaiian Islands to Rarotonga in the Cook Islands. The two terminals of this 4800 km path are very nearly geographic and magnetic dip conjugates, with the magnetic equator very near midpath as shown in Fig. 8. The great circle path is tilted about 10° from the magnetic meridian. This path will be used for the PENEX trans-equatorial experiments. SRI workers used a Granger Associates oblique-incidence sounder transmitter at Kauai and a sounder receiver at Rarotonga. The

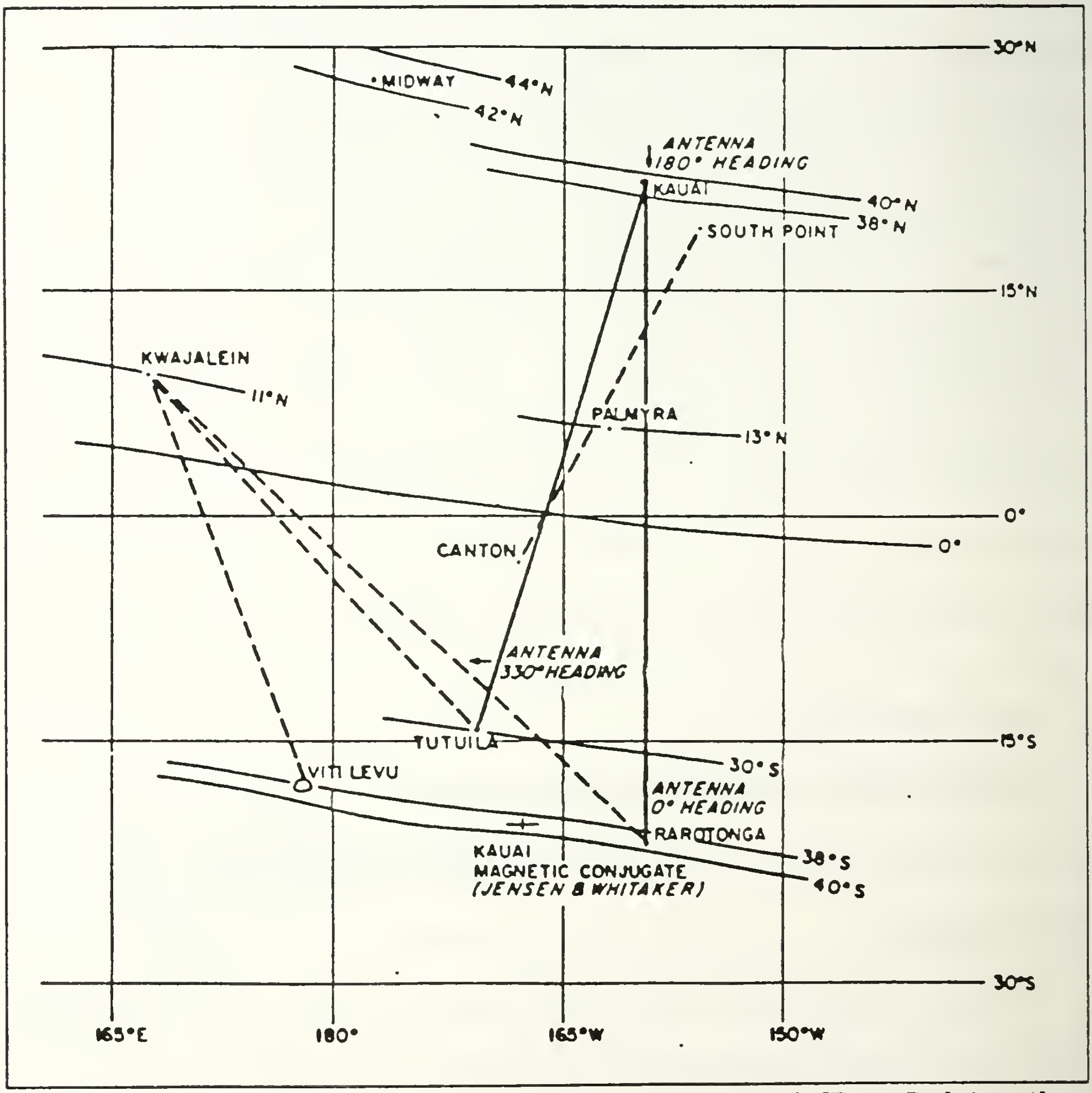

Figure 8. Map Showing Location of Kauai-Rarotonga Path [From Ref. 1: p.4]

sounders swept from 4-64 MHz at various time intervals. Peak-pulse power output was 30 kW, using pulse widths of 100 μs (16 kHz bandwidth) and 1.5 ms (4 kHz bandwidth). SRI used vertically polarized log-periodic antennas with 7-8 dB gain over isotropic and a beamwidth of 110°. [Ref. 1: p.3]

The sounders operated from June through October 1962 providing data for all but a few days of that period. Both the 100 μs and 1.5 ms received signals were recorded on 35-mm film and later digitized to punched card format for their statistical analysis. [Ref. 1: p.5]

C. ANALYSIS OF SRI DATA

1. Time/Frequency Behavior

The propagation frequency spectrum and the percentage of occurrence of propagation on any frequency for one-hour periods are shown in Figs. 9-12. Percentage occurrence is indicated by the length of the horizontal line. A line extending completely across a one hour period indicates 100% occurrence during that month. Also shown are sunrise and sunset times.[Ref. 1: p.6]

Figures 9-12 indicate that the VHF mode is a nocturnal process, commencing generally at sunset, although it occasionally appeared up to two hours before sunset. The average onset time for July and August was 0500Z, and for October and September, 0340Z. It was observed that the normal ($2F_2$, $3F_2$, M, etc.) modes gradually faded out as the VHF mode appeared.[Ref. 1: p.6]

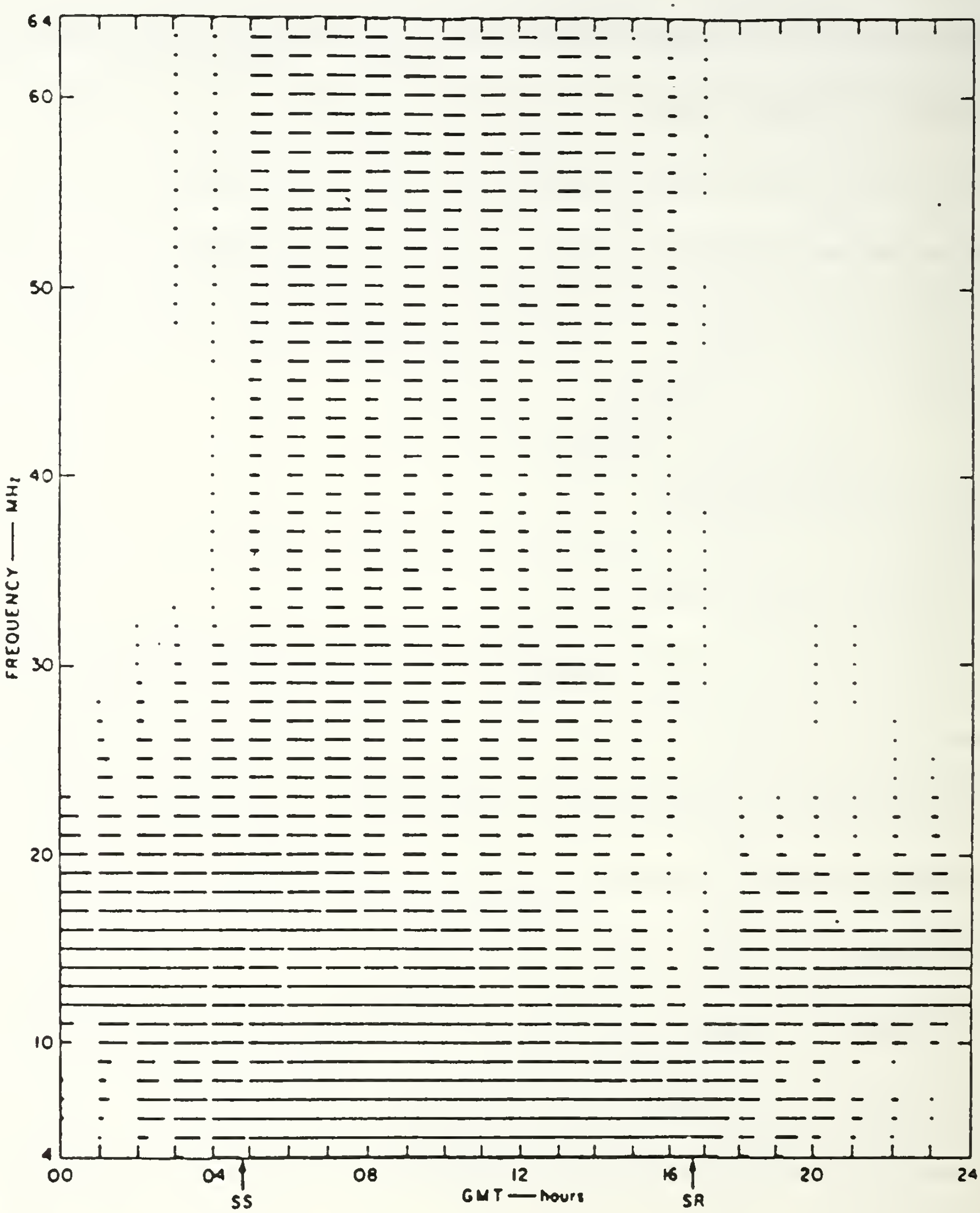

Figure 9. Propagation Spectrum, July 1962 [From Ref 1: p.7]

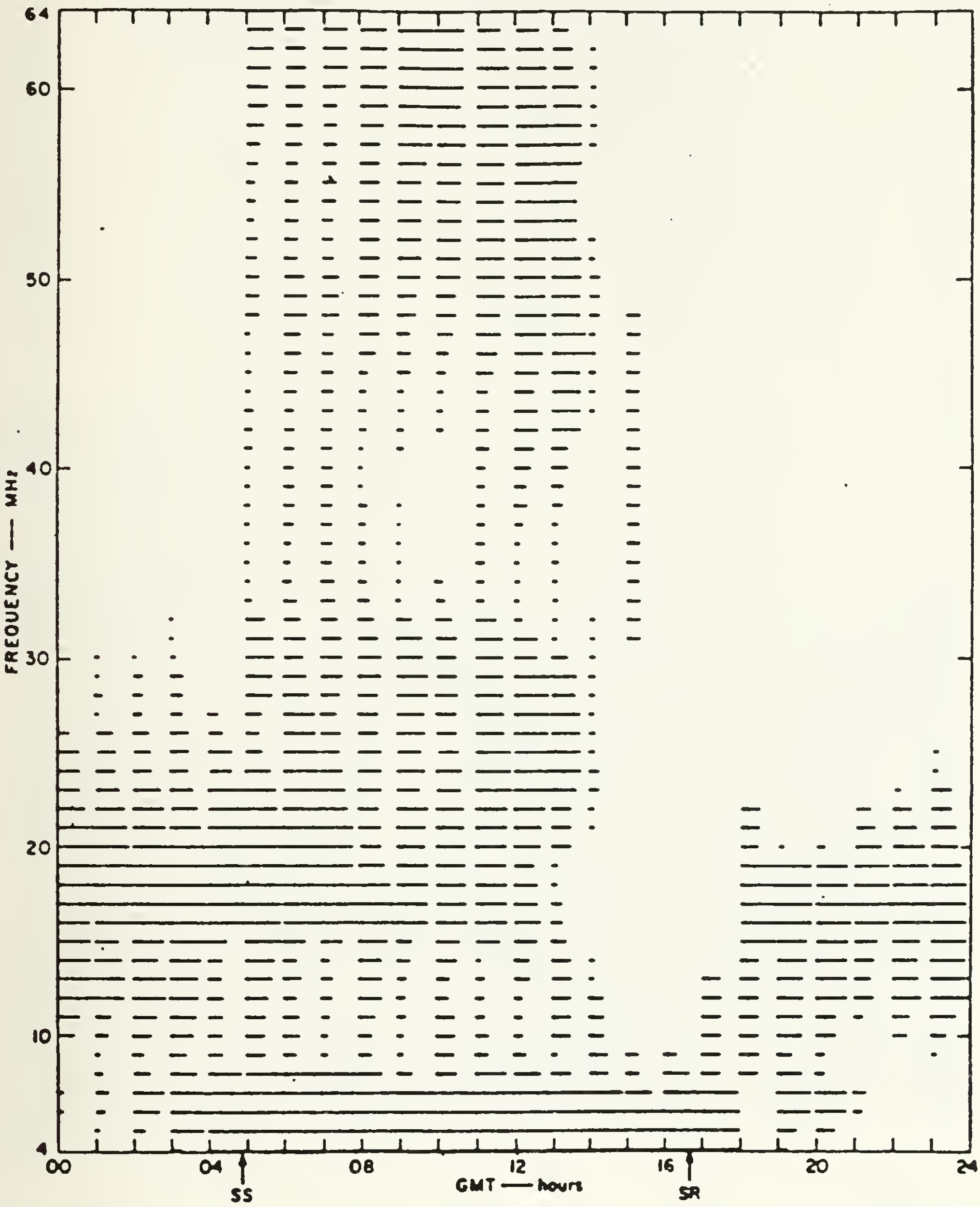

Figure 10. Propagation Spectrum, August 1962 [From Ref. 1: p.8]

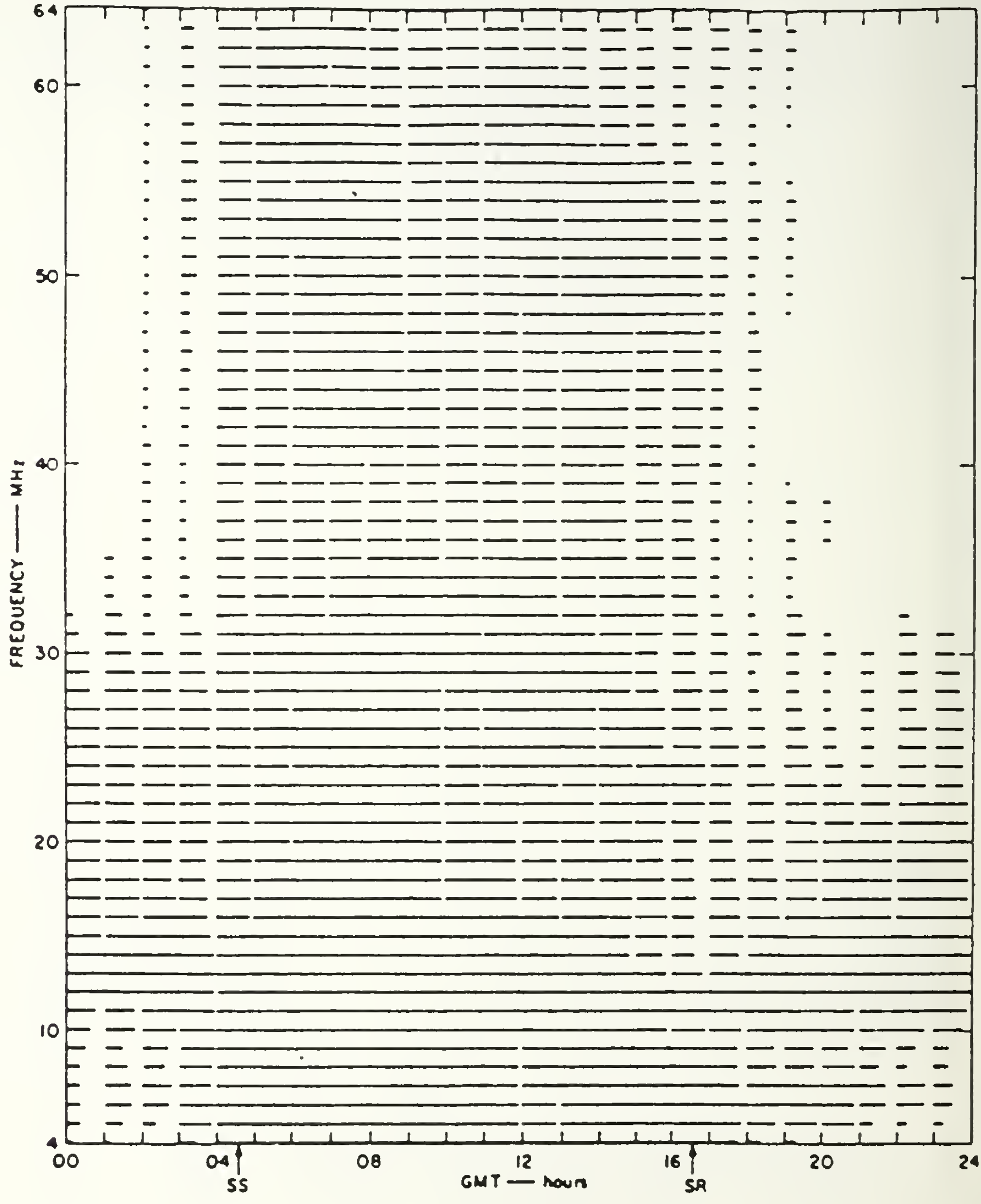

Figure 11. Propagation Spectrum, September 1962 [From Ref. 1: p.9]

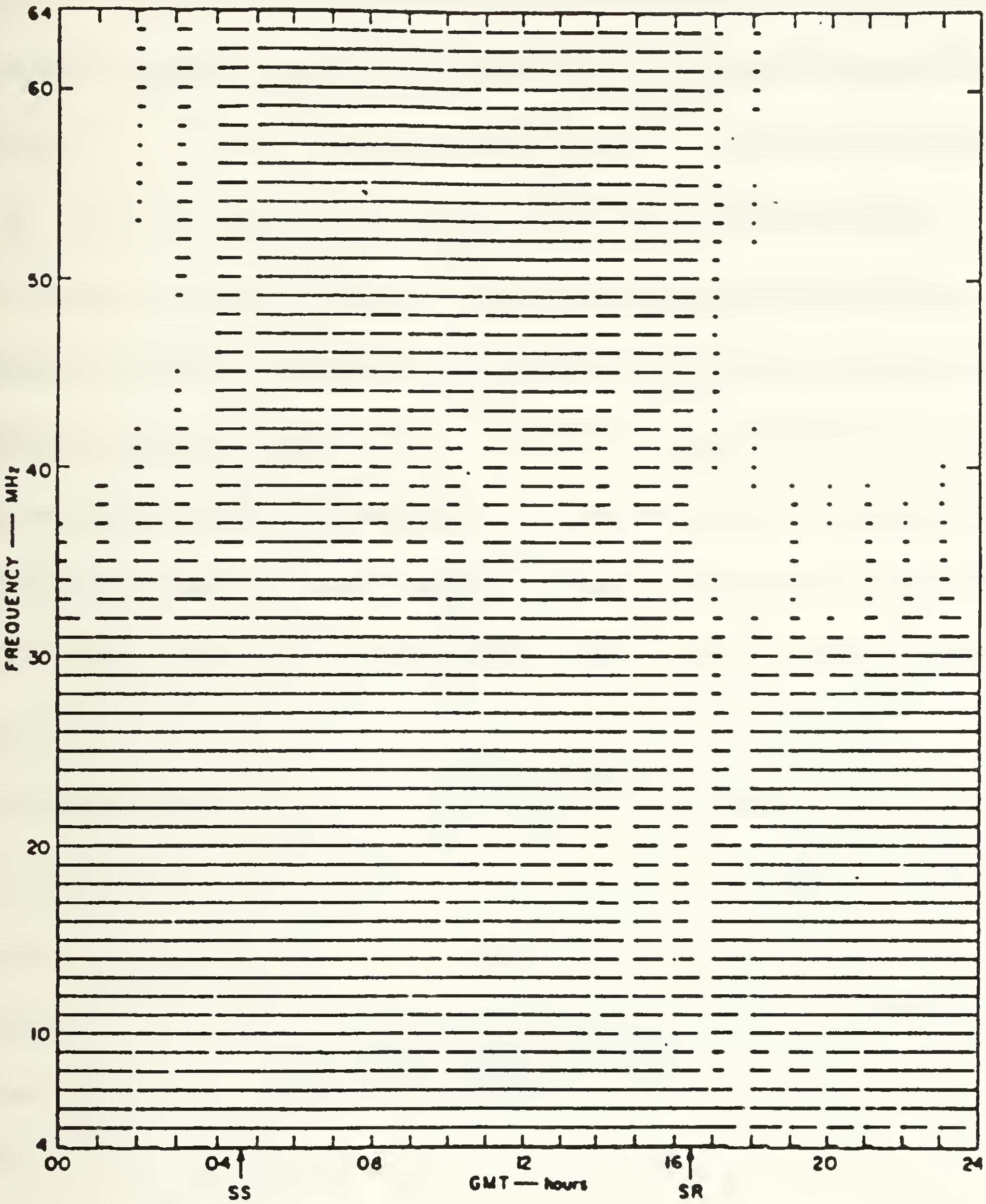

Figure 12. Propagation Spectrum, October 1962 [From Ref. 1: p. 10]

The equinoctial month of October (Fig. 12) reveals that propagation occurred on almost all frequencies from 5-30 MHz nearly 100% of the time, save for two hours after sunrise. Figure 12 also indicates nearly 100% occurrence for 50-64 MHz between sunrise and sunset. Seasonally, then, September/October had a higher percentage of propagation on most frequencies than did July/August.[Ref. 1: p.6]

2. Correlation with Spread F and Magnetic Activity

Geomagnetic activity, as influenced by solar flares and sunspot activity, is known to influence ionospheric phenomena such as spread F. Figure 13 shows the occurrence of the VHF mode on quiet and disturbed days for the summer months of June, July, and August (Fig. 13a) , and the equinoctial months of September, and October (Fig. 13b). The days were selected from the ten quietest and ten most disturbed days of each month based on both K_{psum} and C_p , the magnetic character. The curves of VHF mode

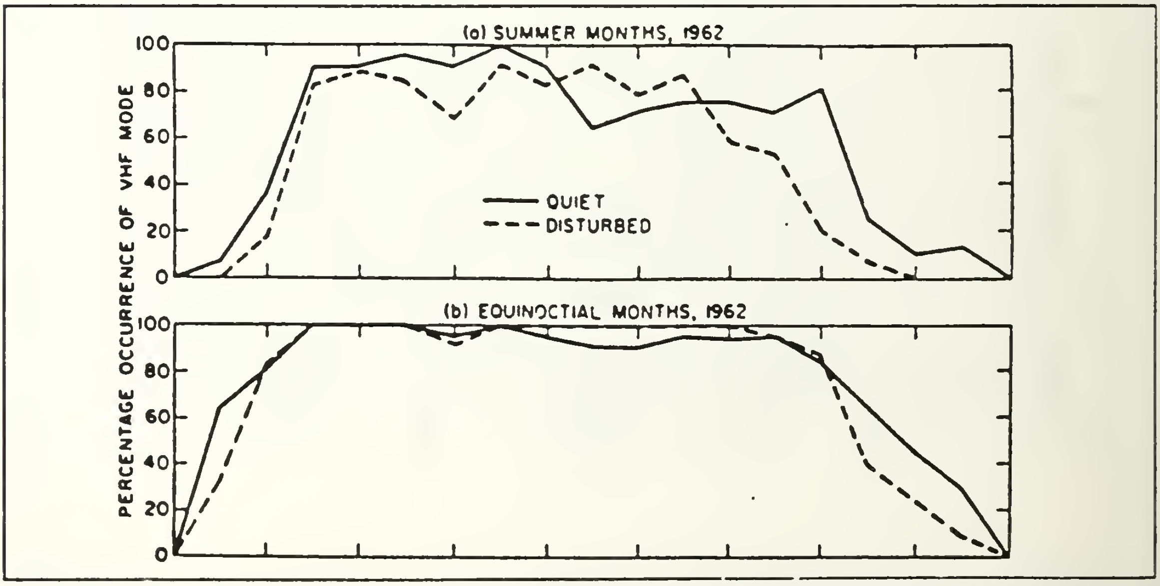

Figure 13. Occurrence of VHF Mode on Quiet and Disturbed Days during the Summer and Equinoctial Months of 1962 [After Ref. 1: p.14]

occurrence exhibit many of the same characteristics of spread-F occurrence. There is a negative correlation with magnetic activity where onset time is earlier on quiet days than on disturbed. Also, seasonally, there are earlier onset times, a higher percentage of occurrence, and longer persistence during the equinoctial months than during the summer months.[Ref. 1: p.13]

3. SRI Conclusions

SRI concluded that only two mechanisms for long range TE propagation of frequencies greater than about 30 MHz could explain their observed anomalies: super mode propagation and the guidance of waves by field-aligned ionization. A super mode would rely upon a pair of local maxima of ionization such as presented by the geomagnetic or Appleton anomaly. This pair, occurring at ± 20° magnetic latitude, allows two ionospheric reflections without a ground reflection. This super mode mechanism is generally observed between 1200-2000 LT; SRI's TE anomalies were nighttime phenomena, occurring at HF down to 4 MHz, so this was probably not the dominant mechanism. Field-aligned ionization at F-region heights, however, is an almost nightly occurrence. To invoke this mechanism, the magnetic field symmetry seems critical -- the dip angle must be just right. Since the terminals of the path were within sight of the equatorial spread-F belt, good coupling into field-aligned irregularities would be possible at altitudes above 200 km with reasonable take-off angles. [Ref. 1: p.33]

D. CONVERSION OF SRI DATA

Data from Figs. 9-12 were converted to surface contour plots for ease of comparison with the AMBCOM predicted spectra. Data was taken from each figure at two hour intervals since this is the interval for propagation chosen for AMBCOM's COMEFF summary report. For each two-hour period, propagation was considered to have occurred if the horizontal line which SRI used to indicate percentage of occurrence was greater than 50% of the two-hour period. Since amplitude data was not available from Ref. 1, contours were constructed for any level of observed propagation. Resulting contour plots, representing the conversion data, are shown in Figs. 14-17. This data will be compared with the predicted propagation patterns in Chapter IV.

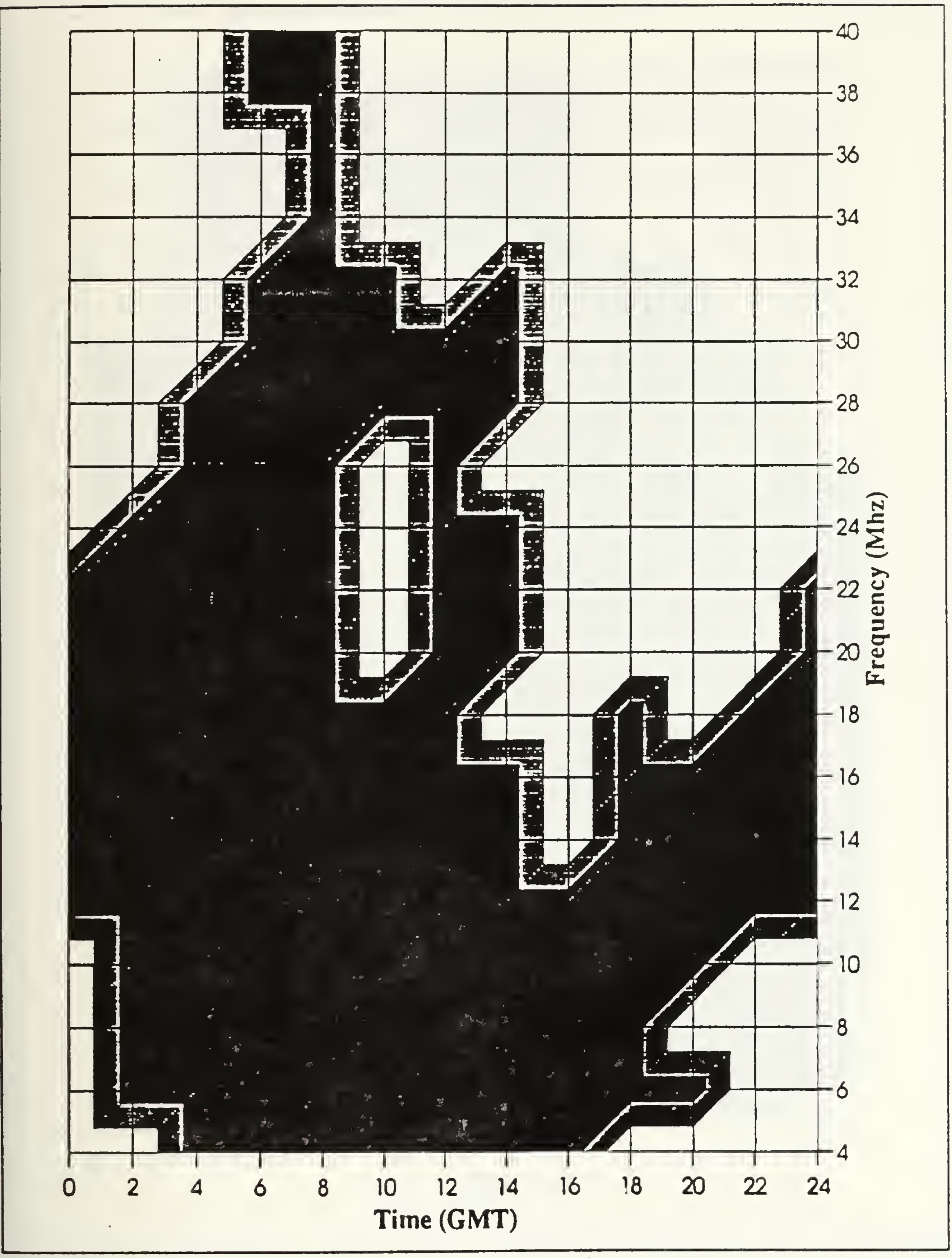

Figure 14. Converted Propagation Spectrum, July 1962

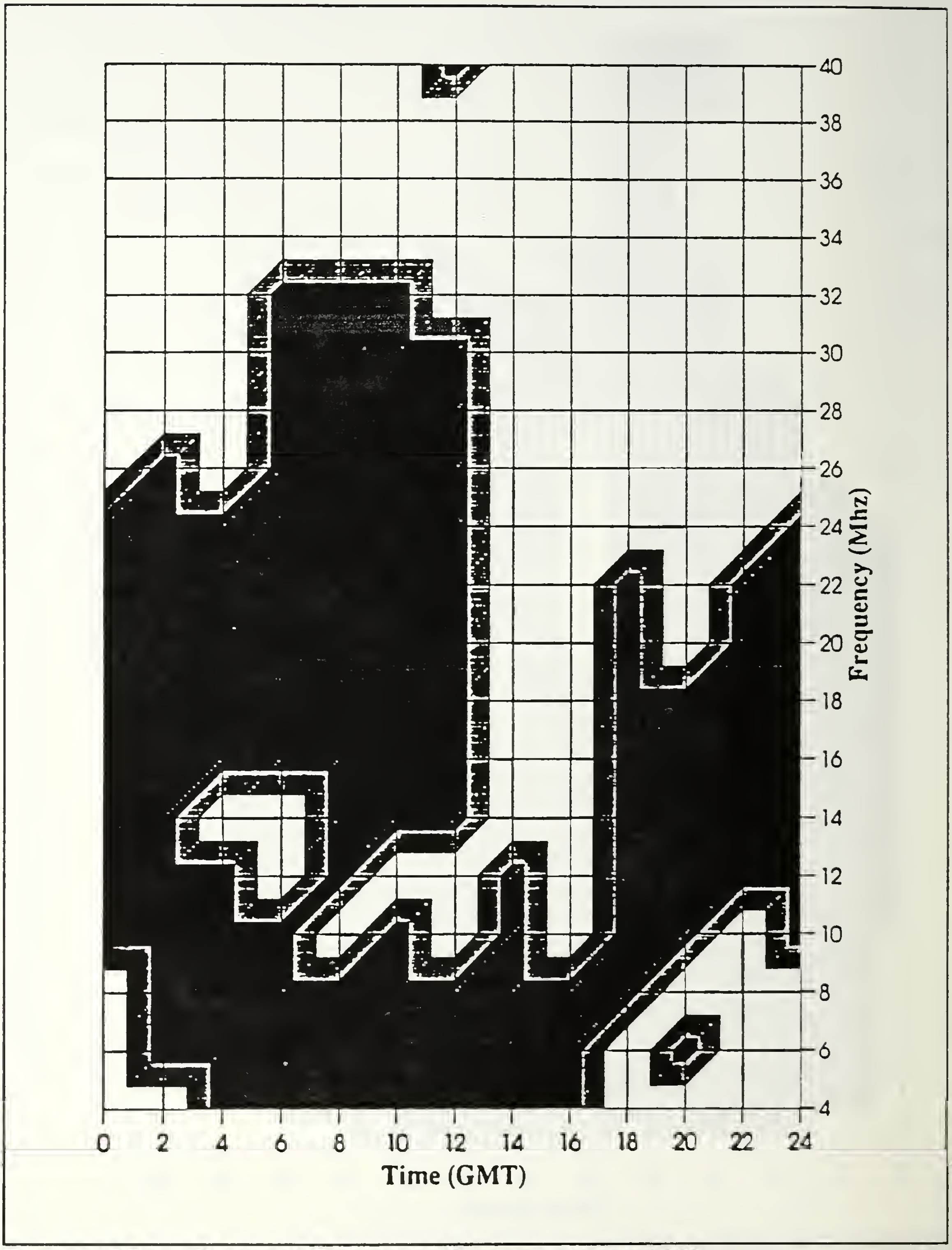

Figure 15. Converted Propagation Spectrum, August 1962

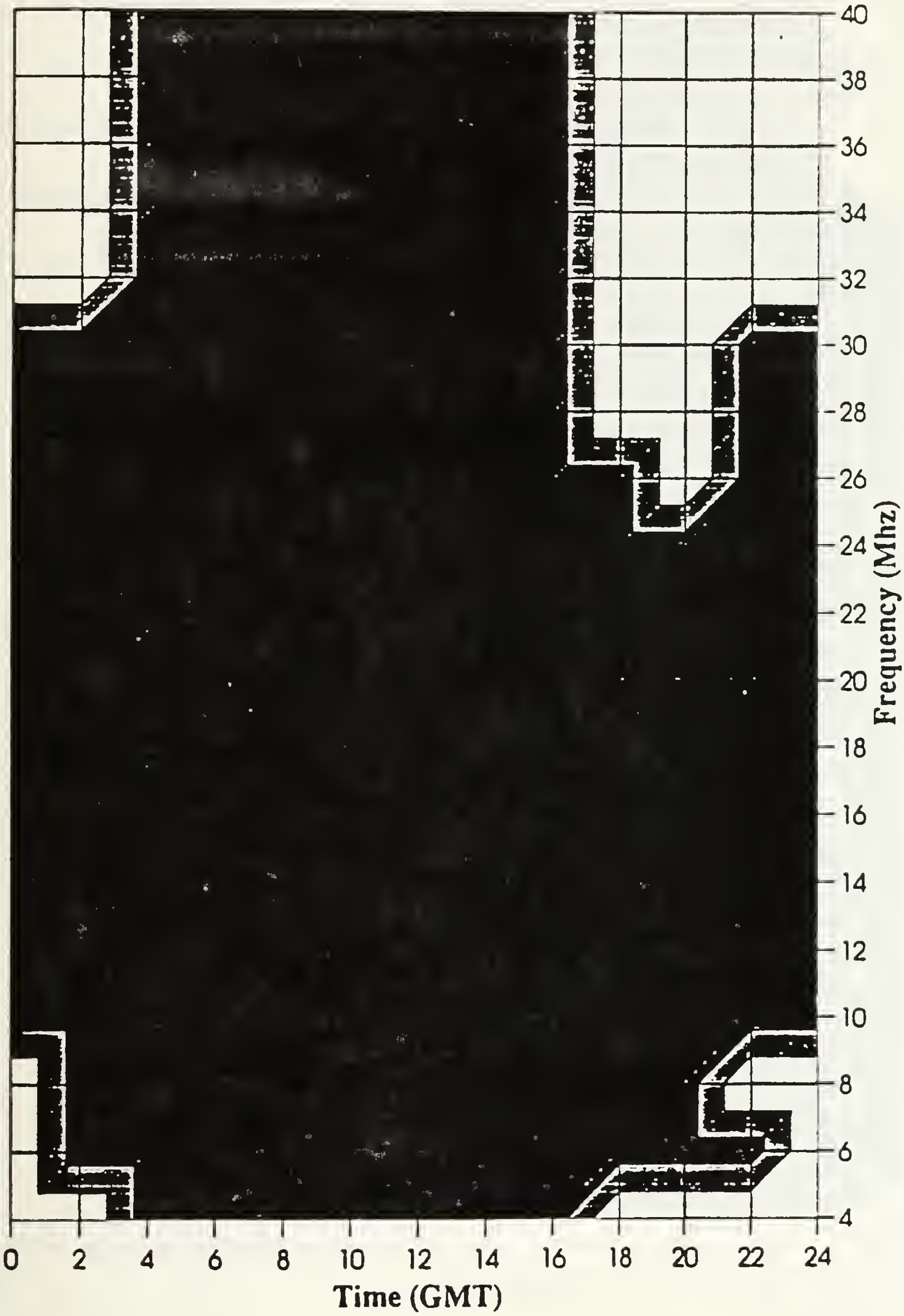

Figure 16. Converted Propagation Spectrum, September 1962

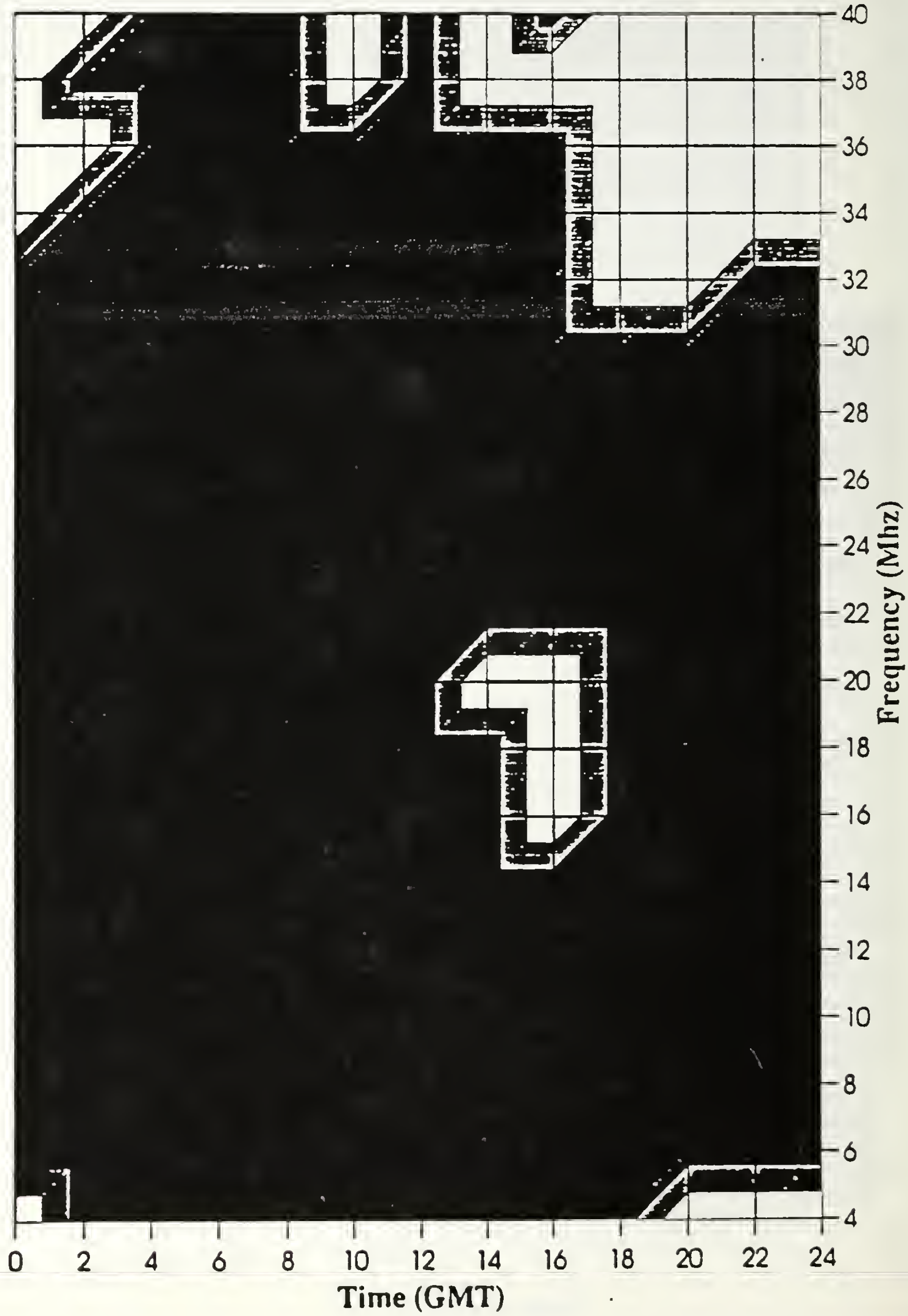

Figure 17. Converted Propagation Spectrum, October 1962

IV. AMBCOM DATA ANALYSIS

A. ANALYSIS METHODOLOGY

AMBCOM's COMEFF program produces a summary table of composite SNR values (in dB), weighted by amplitude of each mode, for all frequencies and times for which calculations were desired. Figure 18 is an example SNR summary table for October 9, 1962. Frequencies were desired from 4-40 MHz; time (GMT) was plotted at two hour intervals. Only those frequencies which supported propagation are presented as output. To produce the data necessary for comparison with the contour plots of the known SRI data, a selectively sampled set of predicted data was desired. From each of

CASE ID: KAUAI-RAROTONGA PATH 9 OCTOBER 1962
P= 0.750E+01 W/HZ BAUD= 0.100E-01 SEC, PLREJ= 8.300E+03 DB
22.00 N 159.50 W HT= 0. -21.20 N 159.80 W HT= 0. 10 42.0 4.2
TRX = ANT726 REC = ANT726 TGT (OPTIONAL) = BEAMWIDTH CORRECTION

FREQ.	TIME (GMT) 0.	2.	4.	6.	8.	10.	12.	14.	16.	18.	20.	22.
4.												
6.			24.	51.	49.	46.	48.	47.	47.	6.		
8.		7.	35.	46.	50.	47.	47.	49.	39.	23.		
10.	7.	22.	44.	43.	52.	52.	51.	39.	18.	32.	16.	6.
12.	19.	31.	42.	50.	53.	53.	52.	44.	41.	28.	27.	20.
14.	26.	33.	49.	55.	53.	54.	37.	10.		38.	30.	25.
16.	25.	27.	51.	54.	52.	53.	39.			3.	33.	28.
18.	44.	44.	47.	52.	46.	40.	47.			46.	31.	24.
20.		45.	46.	49.	46.	42.				45.	18.	7.
22.		44.	44.	48.	46.		20.			41.	30.	42.
24.		45.	45.	47.	48.	19.				45.		
26.	30.	21.	44.	46.	4.	23.				22.		
28.			43.		28.					26.	40.	
30.		37.	43.								42.	42.
32.			14.									37.
34.		3.	19.									
36.		19.									25.	31.

Figure 18. Example SNR table output from COMEFF

the four month's SNR data, the five days exhibiting the most magnetically disturbed character (D in tables of Appendix B) and the five days exhibiting the quietest magnetic character (Q in tables of Appendix B) were grouped separately as samples. SNR values of each month's disturbed days were averaged as were each month's SNR values for quiet days.

An appropriate graphical presentation of the mean SNR values was considered to be a surface-type contour plot, as other three-dimensional graphs, such as histograms, failed to display necessary detail of the data. Data was often not continuous in nature and trends were best observed in the contour plot format.

B. PREDICTED PROPAGATION PATTERNS

Figures 19-26 are contour plots of the mean values of SNR for the disturbed and quiet days for July, August, September, and October 1962. SNR values were grouped in ranges of ten dB; the corresponding contours are shaded with the highest values for SNR displayed darkest. Comparison of these plots with the converted propagation spectrum plots in Chapter three (Figs. 14-17) reveals that AMBCOM poorly predicted observed propagation for all months. However, some trends can be discerned that correspond with SRI's observed trends.

1. July Contour Plots

AMBCOM failed to predict propagation at 4 MHz for all months and only rarely above 32 MHz. It was noted (Figs. 19,20) that AMBCOM failed to predict any of the observed propagation (Fig. 14) between 0500-1600 GMT. The trends before sunset at 0450 GMT and following sunrise at 1645 GMT are predicted fairly well; however, SRI did not observe the predicted propagation at 30-32 MHz around 2400 GMT.

2. August Contour Plots

Predicted propagation for August (Figs. 21,22) extended to higher frequencies (up to 38 MHz) around 2400 GMT. Again, this was not observed by SRI (Fig. 15) The typical null in propagation just before sunrise (1640 GMT) is correctly shown on both predicted and actual plots. Figure 21 for the disturbed August days indicates an erratic patch of propagation at 1800 GMT from 20-22 MHz that SRI also observed. The large area in Figure 15 showing propagation up to 33 MHz from 0500-1300 GMT is not predicted by AMBCOM.

3. September Contour Plots

With the equinoctial months, SRI observed (Fig.16) almost complete propagation. AMBCOM, while indicating much more extensive propagation (Figs. 23,24), fails to fully predict such strong propagation. Erroneously, AMBCOM predicted propagation from 2000-2400 GMT up to 40 MHz, while SRI did not note the same behavior.

4. October Contour Plots

Again, SRI observed nearly complete propagation from 4-40 MHz for the equinoctial month of October (Fig. 17) with a null around sunrise (1620 GMT). AMBCOM predicted this gap (Figs. 25,26), but failed again to predict the propagation from 30-40 MHz.

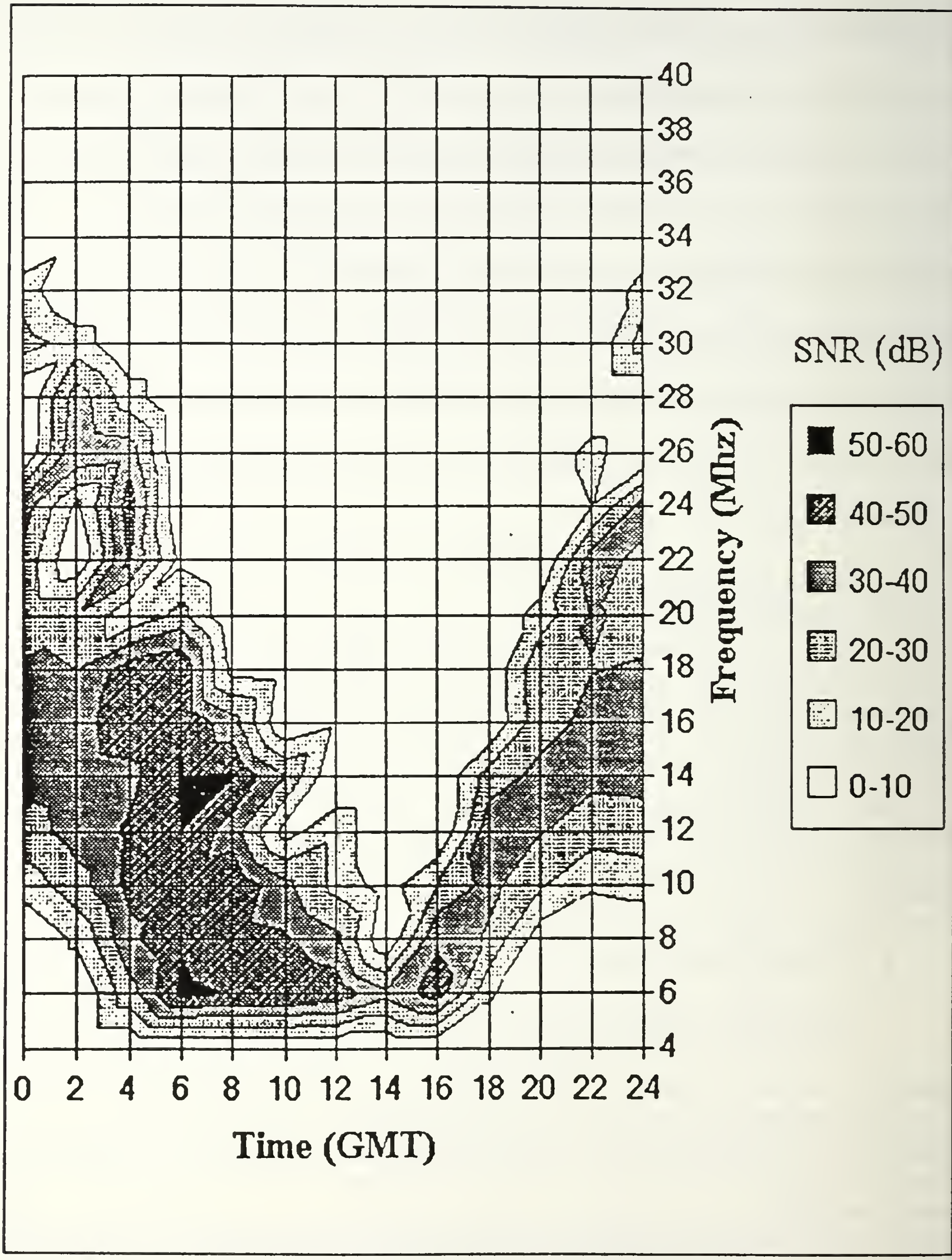

Figure 19. Predicted Propagation Spectrum, July 1962, Disturbed

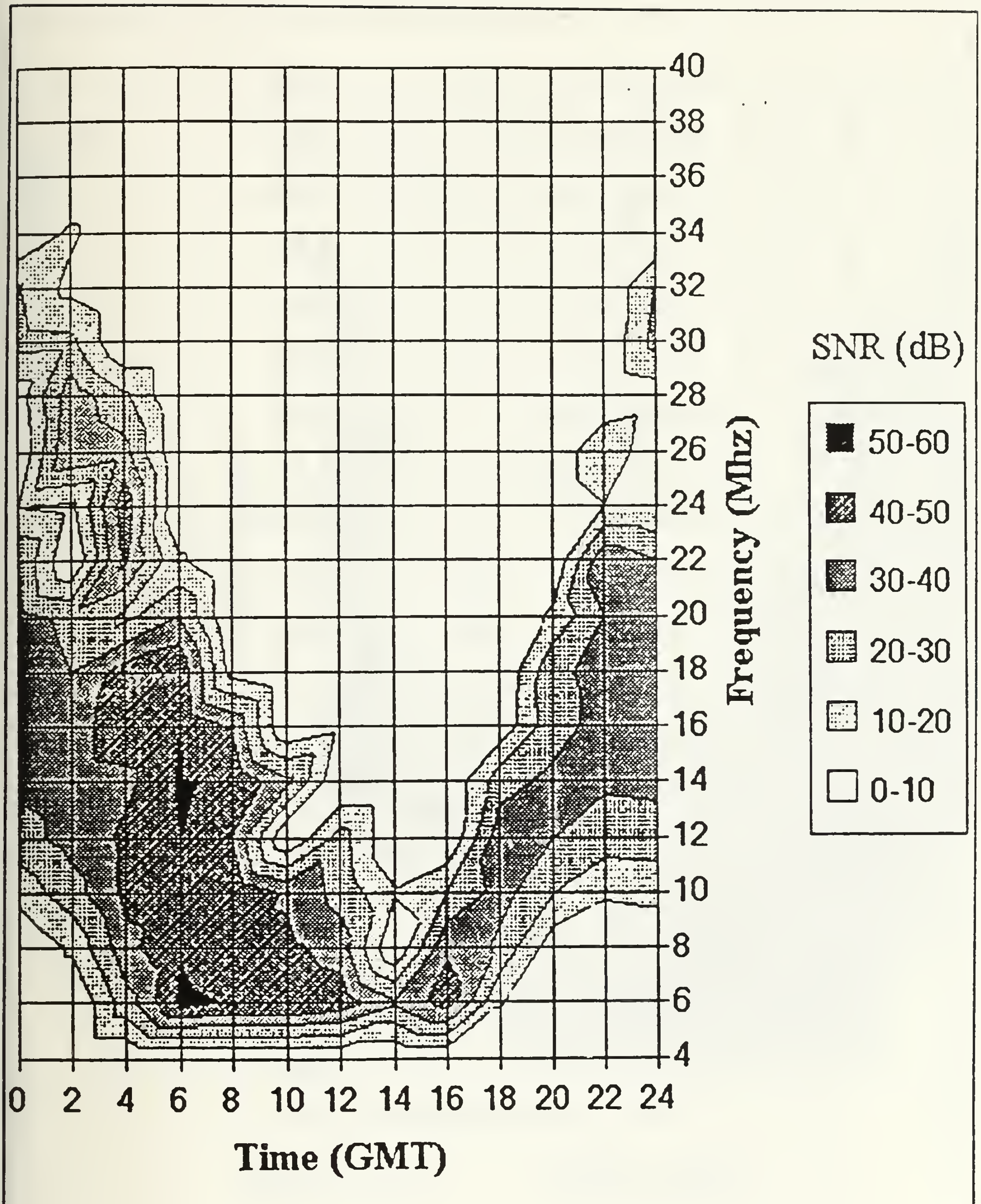

Figure 20. Predicted Propagation Spectrum, July 1962, Quiet

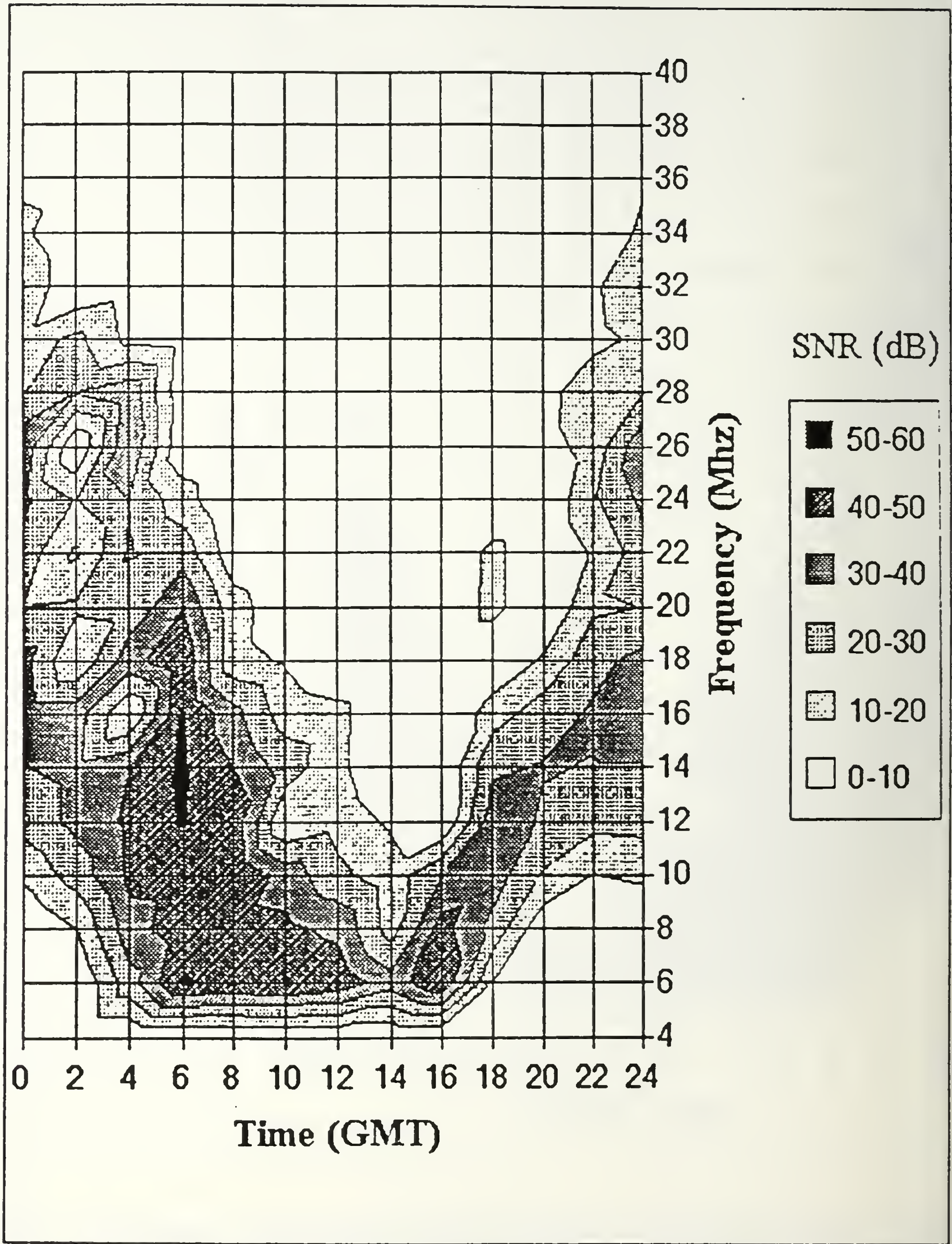

Figure 21. Predicted Propagation Spectrum, August 1962, Disturbed

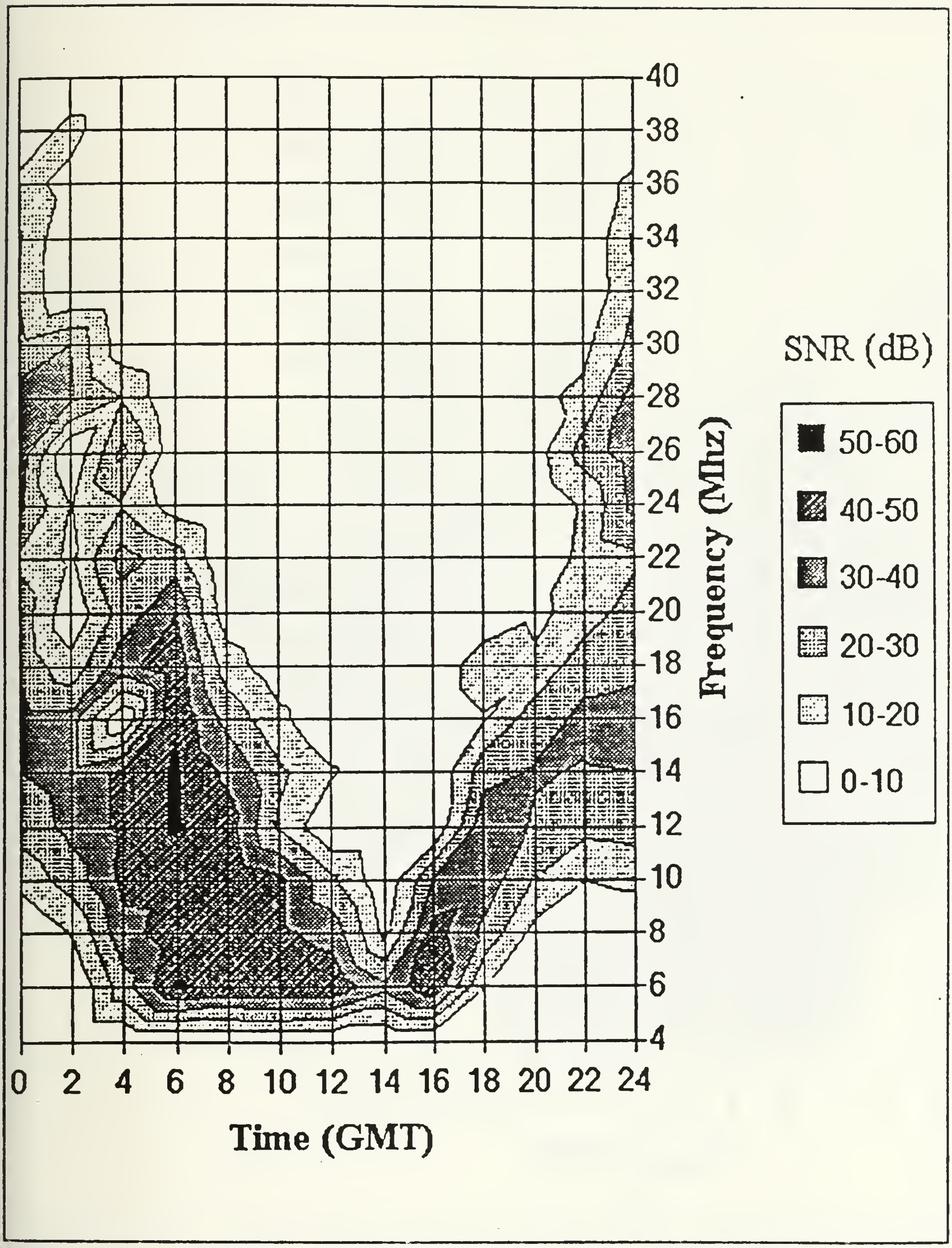

Figure 22. Predicted Propagation Spectrum, August 1962, Quiet

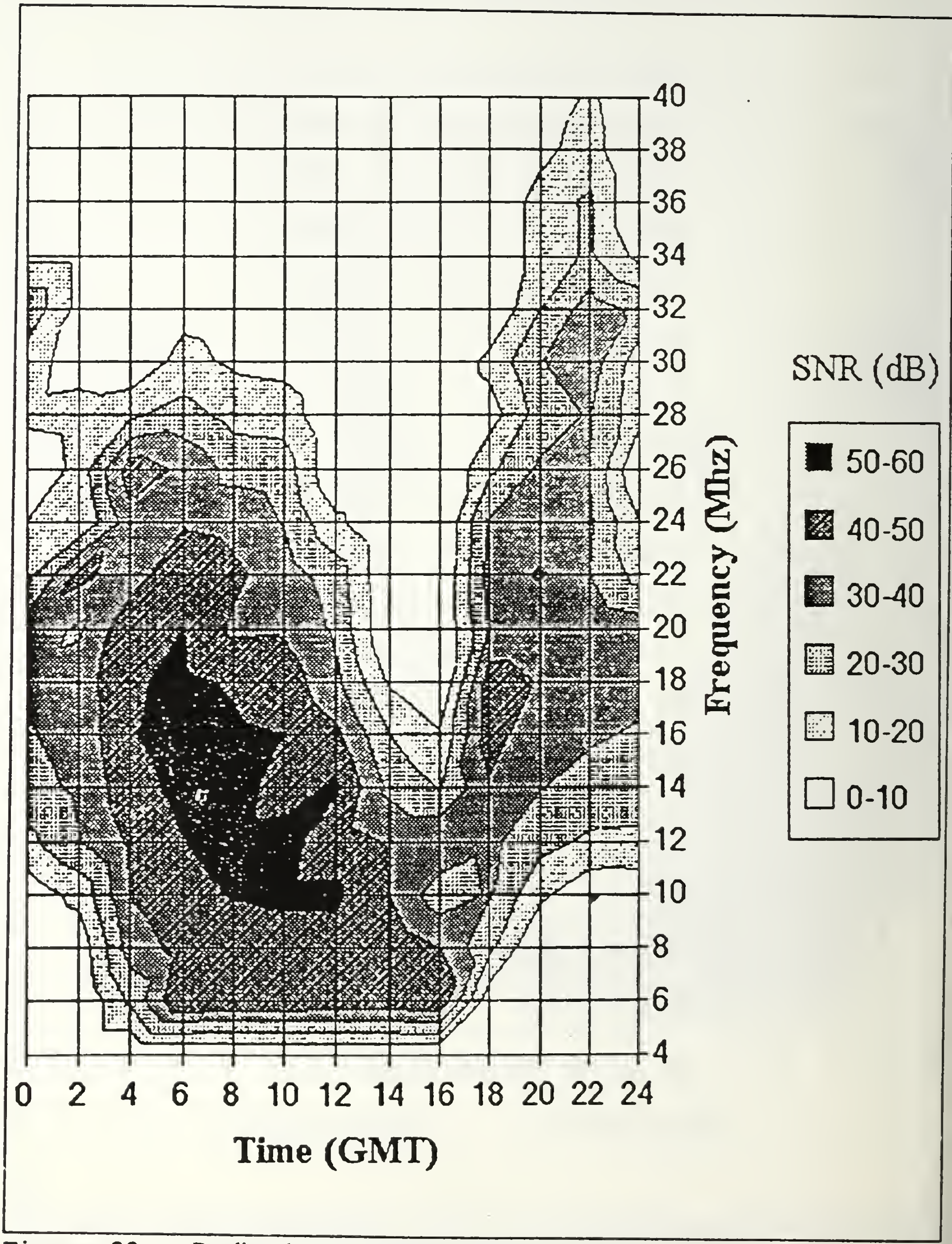

Figure 23. Predicted Propagation Spectrum, September 1962, Disturbed

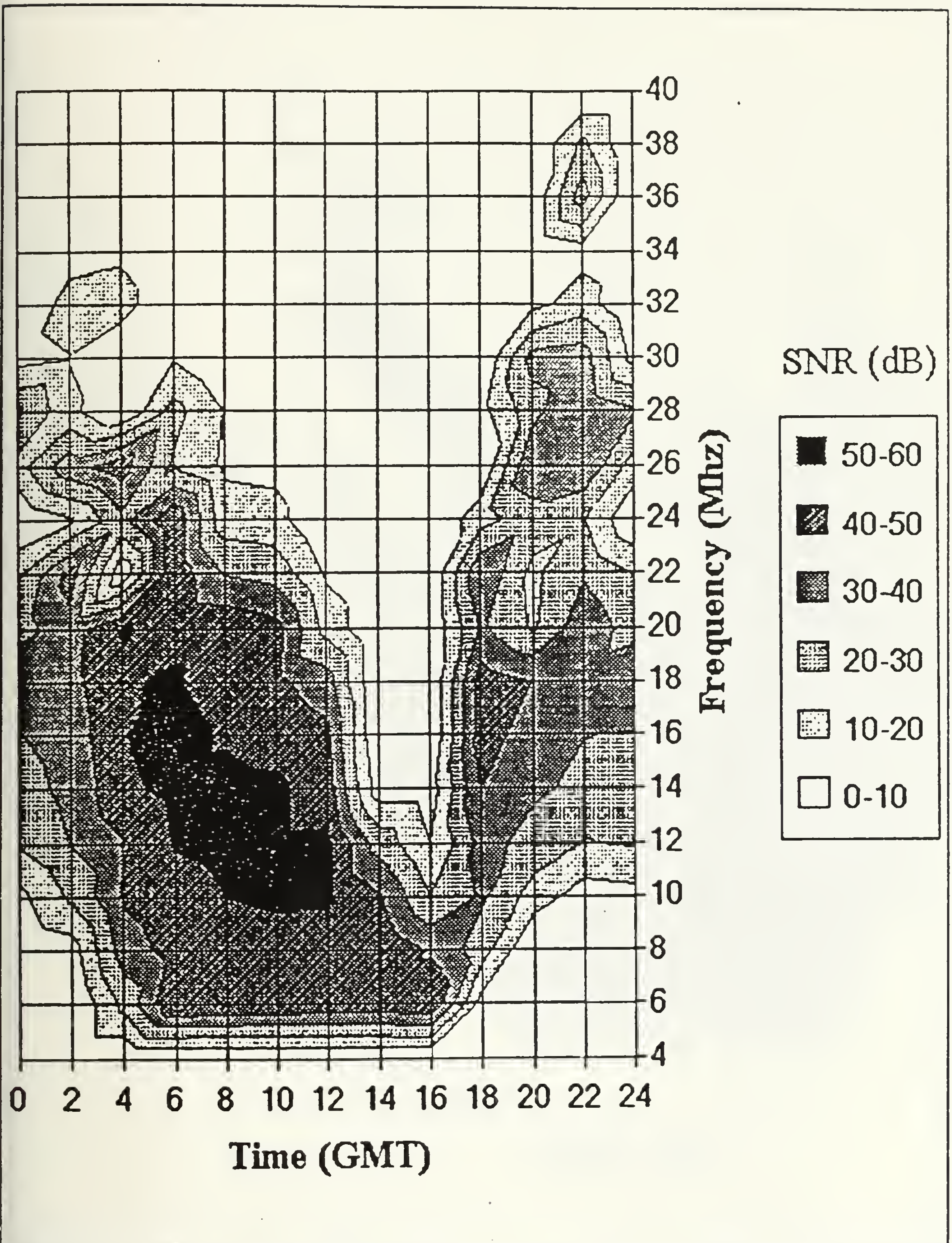

Figure 24. Predicted Propagation Spectrum, September 1962, Quiet

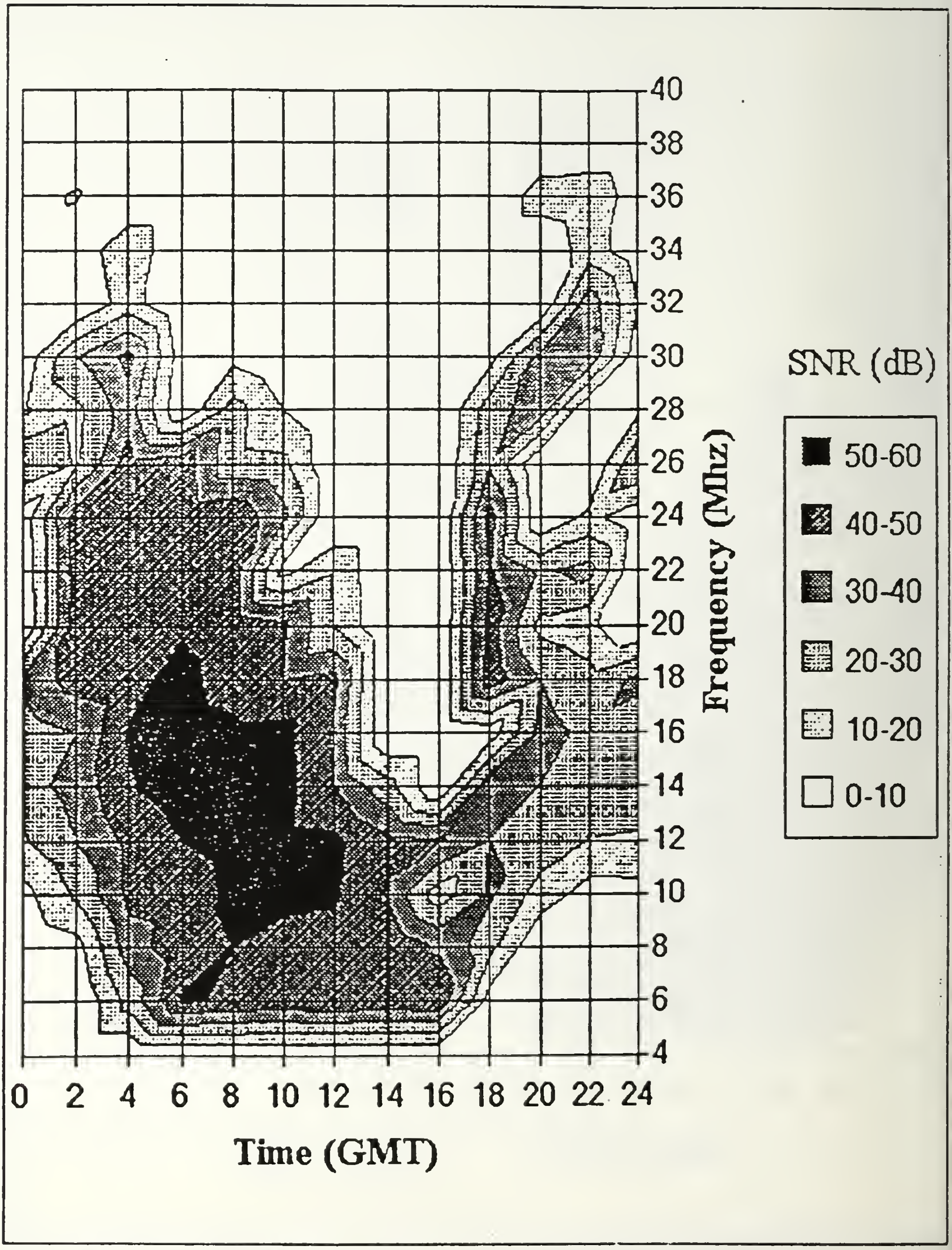

Figure 25. Predicted Propagation Spectrum, October 1962, Disturbed

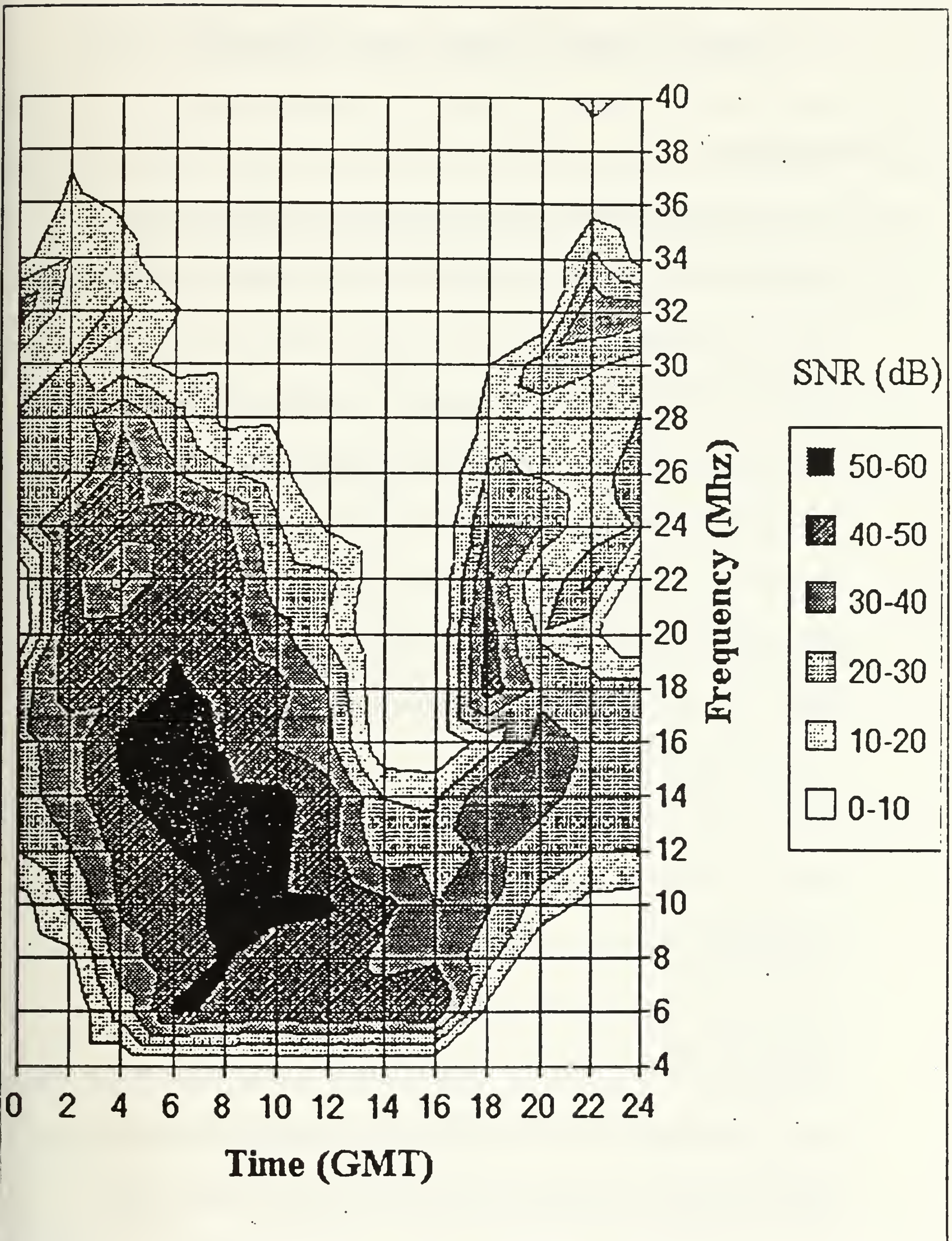

Figure 26. Predicted Propagation Spectrum, October 1962, Quiet

V. CONCLUSIONS AND RECOMMENDATIONS

A. CONCLUSIONS

A number of conclusions were reached during this study, as listed below:

- The bibliography provided at the end of the thesis provided a good background about TE propagation effects.
- The SRI sounder TE data were very useful in obtaining an understanding of TE propagation modes for a magnetic conjugate path. The presence of unusual nocturnal modes were shown to exist.
- This data provided an excellent basis for the comparison of predicted MUF/LUF values to observed MOF/LOF data.
- The SRI data lacked the amplitude information needed for a full evaluation of a TE path for PENEX purposes.
- The comparison of predicted values with observed values indicated significant differences, especially during nighttime hours. This would be expected since the AMBCOM prediction program, and other prediction programs, do not have a routine for the observed TE modes.
- While ANT726 from AMBCOM's ANTLIB.DAT is a vertically polarized log-periodic antenna [Ref. 27], its antenna pattern probably differs from that used by SRI, resulting in differences between predicted and observed data.

B. RECOMMENDATIONS

The AMBCOM program is now available from SRI on PC-based software. The author has not had the opportunity to use this new product. Currently, input control parameters must be located in specific columns, and no data entry programs exist to assist the user in entering these parameters. If data input were changed from the old control card approach to an interactive format for data entry, the program would be much easier to use. Additionally, graphical output displays should be added.

Since sizeable differences were found between the predicted and measured results for this TE path, it is recommended that prediction programs such as AMBCOM, PROPHET, and IONCAP be modified to include the observed TE modes.

APPENDIX A. ANTENNA GAIN TABLE

Table I. GAIN TABLE FOR ANT726, AMBCOM'S VERTICALLY POLARIZED LOG-PERIODIC ANTENNA

GAIN TABLE FOR AMBCOM'S VERTICALLY POLARIZED LOG-PERIODIC
ANTENNA ANT724

FREQUENCY, MHZ

		2	4	6	8	10	12	14	14	18	20	22	24	24	28	30
E	2.0	-10.0	-10.0	-0.1	-1.0	-1.5	-1.5	-1.5	-1.5	-1.5	-1.5	-1.5	-1.5	-1.5	-1.5	-1.5
L	4.0	-10.0	-10.0	3.6	3.2	2.8	2.5	2.3	2.0	1.7	1.5	1.3	1.0	0.8	0.5	0.4
E	6.0	-10.0	-10.0	7.3	7.4	7.1	6.6	6.0	5.5	5.0	6.5	6.0	3.5	3.0	2.5	2.3
V	8.0	-10.0	-10.0	7.5	7.8	7.9	7.8	7.7	7.3	6.6	5.9	5.3	4.6	3.9	3.2	2.9
A	10.0	-10.0	-10.0	7.7	8.2	8.6	9.0	9.3	9.1	8.2	7.4	6.5	5.7	4.8	3.9	3.5
T	12.0	-10.0	-10.0	7.6	8.2	8.8	9.5	10.1	10.1	9.2	8.4	7.5	6.7	5.8	4.9	4.5
I	14.0	-10.0	-10.0	7.1	7.3	7.8	8.4	9.4	9.5	8.8	8.1	7.4	6.7	6.0	5.3	4.9
O	16.0	-10.0	-10.0	6.7	6.5	6.8	7.8	8.7	8.9	8.4	7.8	7.2	6.7	6.1	5.4	5.3
N	18.0	-10.0	-10.0	4.3	5.7	5.9	6.9	7.9	8.3	7.9	7.5	7.1	6.7	6.3	5.9	5.7
	20.0	-10.0	-10.0	4.0	5.2	5.2	4.3	7.3	7.8	7.5	7.2	4.9	4.6	4.3	4.0	5.9
A	22.0	-10.0	-10.0	5.8	4.7	4.4	5.7	4.7	7.2	7.0	4.9	6.7	6.5	4.4	6.2	4.1
N	24.0	-10.0	-10.0	5.5	4.2	4.0	5.0	4.1	6.7	6.4	4.4	6.5	4.4	4.4	6.3	4.3
G	26.0	-10.0	-10.0	5.1	3.9	3.7	4.7	5.8	4.4	4.4	4.4	4.4	4.4	4.4	4.4	4.4
L	28.0	-10.0	-10.0	4.8	3.5	3.3	4.4	5.4	4.2	4.2	4.2	6.2	4.3	4.3	6.3	4.3
E	30.0	-10.0	-10.0	4.7	3.3	3.0	4.1	5.3	5.9	5.9	5.9	5.9	4.0	4.0	6.0	4.0
	35.0	-10.0	-10.0	4.2	2.6	2.0	2.4	3.2	3.4	3.4	3.5	3.5	3.5	3.5	3.5	3.5
I	40.0	-10.0	-10.0	-8.2	-2.4	1.2	2.2	3.1	3.4	3.0	2.7	2.3	1.9	1.4	1.2	1.0
N	45.0	-10.0	-10.0	-4.7	-2.9	-0.6	-0.1	0.3	0.6	0.3	0.2	0.1	-0.1	-0.2	-0.3	-0.4
	50.0	-10.0	-10.0	-4.4	-2.5	-1.3	-0.7	-0.2	0.1	0.0	0.0	-0.1	-0.2	-0.2	-0.3	-0.3
D	55.0	-10.0	-10.0	-4.9	-3.4	-2.3	-1.8	-1.4	-1.1	-1.1	-1.1	-1.1	-1.2	-1.2	-1.2	-1.2
E	60.0	-10.0	-10.0	-5.4	-4.2	-3.3	-2.9	-2.5	-2.3	-2.3	-2.2	-2.2	-2.2	-2.1	-2.1	-2.1
G	45.0	-10.0	-10.0	-5.8	-5.0	-4.3	-4.0	-3.7	-3.5	-3.4	-3.3	-3.3	-3.2	-3.1	-3.0	-3.0
R	70.0	-10.0	-10.0	-6.3	-5.8	-5.4	-5.1	-4.8	-4.6	-4.5	-4.4	-4.3	-4.2	-6.1	-4.0	-3.9
E	75.0	-10.0	-10.0	-6.7	-6.6	-6.6	-6.2	-6.0	-5.8	-5.7	-5.5	-5.4	-5.2	-5.0	-4.9	-4.8
E	80.0	-10.0	-10.0	-7.2	-7.4	-7.4	-7.3	-7.2	-7.0	-6.8	-6.6	-6.4	-6.2	-6.0	-5.8	-5.7
S	85.0	-10.0	-10.0	-7.6	-8.2	-8.5	-8.6	-8.3	-8.2	-7.9	-7.7	-7.5	-7.2	-7.0	-6.7	-4.6
	90.0	-10.0	-10.0	-8.1	-9.0	-9.5	-9.5	-9.5	-9.4	-9.1	-8.8	-8.5	-8.2	-7.9	-7.4	-7.5
	LOSS	99.0	99.0	0.0	0.0	0.0	0.0	0.0	0.0	0.0	0.0	0.0	0.0	0.0	0.0	0.0
	BWIDTH	340.0	340.0	110.0	110.0	110.0	110.0	110.0	110.0	110.0	110.0	110.0	110.0	110.0	110.0	110.0

APPENDIX B. GEOMAGNETIC AND SOLAR DATA TABLES

The data contained in the following tables is compiled monthly in the *Journal of Geophysical Research* as Geomagnetic and Solar Data, J. Virginia Lincoln, Editor [Refs. 4-7]. Last column annotations denote Q/q - 10 quiet days, Q - 5 quiet days, D - 5 disturbed days.

Table II. GEOMAGNETIC AND SOLAR DATA, JULY 1962

	Kp (3-hour intervals)								Sum	Ave.		
Day	1	2	3	4	5	6	7	8	Kp	Kp	Rz	Q/D
1	2o	2o	3-	3o	2+	2+	2-	2o	18o	2.3	54	
2	2+	1o	2o	2o	1-	2-	3-	3o	15+	1.9	39	q
3	3-	1o	2-	2o	2o	3-	2+	1+	16-	2	38	q
4	2o	4-	3o	2+	3+	2o	4+	5-	25+	3.2	30	D
5	3o	4o	4o	3o	2+	2+	3+	2+	24+	3	26	D
6	3+	3o	3-	4-	2o	2-	2+	2o	21-	2.6	20	
7	1o	1-	1-	2+	2-	2+	3o	3+	15o	1.9	21	
8	2o	3o	3o	2+	2o	2o	2+	3o	20-	2.5	16	
9	2+	2o	2o	1+	1-	1-	1+	2-	12o	1.5	10	Q
10	2o	1o	1+	0+	3o	3+	2o	2o	15o	1.9	13	
11	2o	2-	3-	2o	3-	2+	3-	2+	18+	2.3	19	
12	1o	3o	2+	2o	2o	2o	1+	1+	15o	1.9	11	q
13	3o	1+	2-	1+	3-	3-	3o	3o	19-	2.3	29	
14	3o	3-	3-	2-	2-	2+	1o	2o	17o	2.1	33	
15	3o	1o	1-	1-	1-	1+	2o	2o	11o	1.4	21	q
16	2o	1+	0+	0+	1o	0+	0+	0o	6-	0.7	26	Q
17	0+	0+	0+	0+	1-	0+	0+	1o	4-	0.5	31	Q
18	1+	1-	1-	1-	1+	1-	2o	1o	8+	1	29	Q
19	1+	2+	2o	3o	2+	1+	3+	3-	18+	2.3	8	
20	3+	4o	4o	3-	2+	3-	3-	2o	24-	3	14	
21	3o	3-	2-	3-	2o	3o	2+	3o	21+	2.7	23	
22	3o	2o	2+	2-	1-	1+	1+	2o	14+	1.8	23	q
23	1o	2+	3o	2o	1+	1o	3+	2-	16-	2	17	
24	2+	1o	1o	1-	2o	4+	5-	4o	20o	2.5	13	
25	5-	4+	3+	2+	2-	1-	1o	2+	20+	2.5	11	
26	3-	6+	6-	6-	5o	3+	4+	4+	37+	4.7	9	D
27	5o	4-	3+	3-	4o	5+	3-	4o	31-	3.8	9	D
28	4-	4-	4o	3-	3o	4-	2+	3-	26-	3.2	9	D
29	4-	2-	3o	2-	+	3-	1+	2-	17o	2.1	8	
30	2o	3-	2o	0+	1-	1-	1-	1+	10+	1.3	7	Q
31	1-	1-	1+	1+	1-	2o	4+	4+	15+	1.9	0	

Table III. GEOMAGNETIC AND SOLAR DATA, AUGUST 1962

	Kp (3-hour intervals)								Sum	Ave.		
Day	1	2	3	4	5	6	7	8	Kp	Kp	Rz	Q/D
1	5o	5+	5-	6o	4-	3o	3o	4o	35-	4.3	0	D
2	3+	3o	1o	2+	2+	2+	2+	2o	19-	2.3	7	
3	2o	3-	3-	2-	3-	3-	3-	3-	20-	2.5	7	
4	1o	2o	2+	2-	2-	2-	2+	1+	14o	1.8	10	q
5	2o	2o	3-	3o	2o	2-	1+	1-	15+	1.9	14	q
6	3o	3+	4o	3o	4-	3+	3-	3+	26+	3.3	11	
7	4o	3o	2+	2+	3o	4-	5-	4+	27+	3.5	9	
8	5o	4o	5o	4+	4o	4o	3-	4+	33+	4.2	8	D
9	5-	3+	4o	3+	3o	2+	3-	3o	26+	3.3	0	
10	3o	3-	3+	2+	2+	3-	1o	1o	18+	2.3	0	
11	1o	1-	0+	0+	1-	0+	1-	0o	4o	0.5	0	Q
12	0+	1o	1-	2-	2-	0+	0+	1o	7o	0.9	15	Q
13	1-	1-	1o	1+	1-	0+	1o	3+	9o	1.1	24	Q
14	2+	2+	1o	2-	2+	1o	3o	3+	17o	2.1	40	
15	3-	5-	5o	3+	2o	3-	3-	4o	27o	3.4	50	
16	5o	3+	4o	1o	1+	2-	4-	5-	25-	3.1	50	
17	4+	3+	3o	3o	3+	4-	4-	5o	29+	3.7	53	D
18	3+	4+	5-	3-	3+	4-	2+	3+	28-	3.5	43	
19	4+	4+	3+	3+	3-	2+	2o	2+	25-	3.1	45	
20	2-	1-	1o	1+	2-	1o	1-	2-	10-	1.2	39	Q
21	2o	1-	1-	1o	1o	2-	1+	4-	12o	1.5	36	q
22	5+	4o	5+	2+	3-	3-	5-	5-	32-	4	30	D
23	4-	3+	3o	3+	3+	3+	3o	3-	26-	3.2	27	
24	3+	3o	4+	3+	4+	3+	2+	4-	28-	3.5	30	
25	4o	3-	3o	2+	2o	3-	2o	3+	22o	2.8	14	
26	3-	2+	2+	3-	2+	1o	1o	1o	15+	1.9	7	q
27	2+	2o	2+	0+	0+	1-	1o	1-	10-	1.2	7	q
28	1+	2o	1-	2-	2-	1+	0+	0+	9+	1.2	14	Q
29	1o	3o	3+	4-	3-	3-	3+	3+	23o	2.9	8	
30	2+	3o	3-	2-	4-	3-	4-	2o	22-	2.7	25	
31	5-	5-	5+	4-	3+	1+	3-	2o	28-	3.5	22	D

Table IV. GEOMAGNETIC AND SOLAR DATA, SEPTEMBER 1962

	Kp (3-hour intervals)								Sum	Ave.		
Day	1	2	3	4	5	6	7	8	Kp	Kp	Rz	Q/D
1	3+	2+	5-	4o	4o	5o	5-	4o	32o	4	48	
2	3o	5-	5-	5-	6-	4o	4+	3+	34+	4.3	57	D
3	4o	5+	4-	5+	4o	4o	6-	6+	38+	4.8	81	D
4	5-	6-	4+	5-	4o	5o	4-	3o	35o	4.4	88	D
5	1o	3+	4o	3+	3o	4-	3-	3o	24o	3	90	
6	4-	4o	5o	4o	3-	2o	3o	3+	28-	3.5	82	
7	4-	4-	4o	3o	3-	1+	2o	1+	22-	2.7	71	
8	3+	4o	4o	3o	2-	2o	1o	2-	21-	2.6	59	
9	3-	3o	1-	2o	2+	2o	3o	3+	19o	2.4	58	
10	3o	4o	3-	3o	2-	1-	1-	1o	17-	2.1	44	q
11	2+	1+	2+	4-	1-	1-	2-	3-	15+	1.9	51	q
12	3-	3o	7+	5o	4-	5-	7-	6-	39-	4.8	62	D
13	4o	3+	4-	3-	3o	4+	5o	2o	28o	3.5	59	
14	3o	3o	4o	2-	1o	2-	2o	2+	19-	2.3	53	q
15	3o	4-	4o	3-	1-	2+	3+	3o	23-	2.8	60	
16	2+	3-	1-	2o	2o	2-	3o	3+	18-	2.2	42	q
17	2o	3-	2+	1+	2o	1+	2-	2o	15+	1.9	33	Q
18	2-	1-	1o	1o	1o	1o	1+	3-	10+	1.3	35	Q
19	3o	4+	6-	4o	3+	4+	6o	5-	35+	4.4	24	D
20	5-	3+	2+	4-	2+	1-	1o	1-	19-	2.3	24	
21	2o	3-	3-	2-	3o	4-	3-	3-	21o	2.6	32	
22	4o	4-	3o	4o	4-	4-	4-	2+	28o	3.5	32	
23	3+	4+	3o	3+	1+	1o	1+	2+	20o	2.5	41	
24	2+	3o	1o	0+	1-	0+	2o	2-	11+	1.4	54	Q
25	0+	1-	1-	2-	2-	2+	2+	3-	13-	1.6	53	Q
26	5+	6-	3+	2o	3+	5+	4o	2+	31+	3.9	55	
27	3o	2+	2o	2+	3-	2o	1o	2-	17o	2.1	51	q
28	3-	1+	1-	1o	2+	3-	2-	3+	16-	2	47	Q
29	2o	3+	3o	3+	2+	2+	3+	5+	25o	3.1	36	
30	4o	4+	3o	3-	3-	2o	2-	1+	22-	2.7	46	

Table V. GEOMAGNETIC AND SOLAR DATA, OCTOBER 1962

	Kp (3-hour intervals)								Sum	Ave.		
Day	1	2	3	4	5	6	7	8	Kp	Kp	Rz	Q/D
1	3+	4+	5o	5o	5+	5-	6-	5-	38o	4.8	51	D
2	4+	4-	5-	4-	4-	4+	3-	1+	28+	3.5	35	
3	2-	2-	4-	2+	3+	2-	2-	3-	20-	2.5	22	q
4	2+	3+	3o	2o	1-	2+	2o	3-	18+	2.3	18	Q
5	1o	2-	1+	1o	1+	3-	5-	3+	17o	2.1	13	q
6	5-	4-	4+	1o	3+	3-	0+	2+	22+	2.8	25	
7	2+	3+	1+	2o	1-	1+	3+	4+	19-	2.3	37	q
8	6+	4-	3+	4+	3+	5-	4o	4o	34-	4.2	40	D
9	6-	4+	5-	4-	4+	4o	3o	4-	33+	4.2	42	D
10	4-	3+	3-	3+	5-	4-	4+	3-	28+	3.5	51	
11	4-	5o	4+	3+	4-	3o	4-	3+	30o	3.8	63	
12	3o	2+	2+	4-	2-	1+	1-	1-	16-	2	63	Q
13	1-	1+	1+	3+	4-	3-	2+	3o	18+	2.3	74	q
14	4o	4+	5-	5-	4o	3o	5-	4-	33o	4.1	67	
15	3-	3+	2+	3-	2-	3-	1-	2o	18o	2.3	62	Q
16	3-	2o	2o	6-	4o	2o	4-	3o	25o	3.1	51	
17	3+	2+	3-	2o	1-	0o	1o	1+	13+	1.7	43	Q
18	5-	5-	2-	1+	2-	3+	3o	1+	22-	2.7	33	
19	0+	0o	5o	5o	5-	5o	4-	4-	27+	3.4	29	
20	2o	2o	2-	1o	3-	3-	3o	4-	19-	2.3	28	q
21	4-	3+	2+	2+	2o	4-	3o	2o	22+	2.8	35	
22	2+	4-	3o	4o	4+	3+	3+	5-	29-	3.6	41	
23	5o	4o	3o	4-	3+	4-	3o	3+	29o	3.6	43	
24	3o	4-	3-	3o	4o	5o	5-	5-	31-	3.8	41	
25	4-	4+	4+	4o	4+	5-	5-	5o	35o	4.4	43	D
26	4-	4-	5-	4+	4+	4+	5+	4o	34+	4.3	48	D
27	4-	4o	5o	3o	5o	5-	3-	3+	31+	3.9	42	
28	3+	4+	3+	3o	3o	3-	3+	3o	26o	3.3	31	
29	3o	3-	3-	3-	2+	3-	2+	3+	22-	2.7	15	
30	3o	3o	3o	3+	2+	3o	3+	2+	23+	2.9	20	
31	2o	2+	2+	3-	2o	2-	2+	3-	18o	2.3	23	Q

LIST OF REFERENCES

1. Nielson, D.L., and Bartholomew, R.R., "VHF propagation over a 4800-Km transequatorial path," Stanford Research Institute, Menlo Park CA, June 1966.

2. Goodman, J.M., *HF Communication, Science & Technology*, Van Nostrand Reinhold, 1992.

3. Davies, K., *Ionospheric Radio*, Peter Peregrinus, Ltd., London, United Kingdom, 1990.

4. Lincoln, J.V., "Geomagnetic and Solar Data," *J. Geophys. Res.*, v.67, n.12, p.4877, Nov. 1962.

5. Lincoln, J.V., "Geomagnetic and Solar Data," *J. Geophys. Res.*, v.67, n.13, p.5342, Dec. 1962.

6. Lincoln, J.V., "Geomagnetic and Solar Data," *J. Geophys. Res.*, v.68, n.2, p.585, Jan. 1963.

7. Lincoln, J.V., "Geomagnetic and Solar Data," *J. Geophys. Res.*, v.68, n.4, p.1156, Feb. 1963.

8. McNamara, L.F., *The Ionosphere: Communications, Surveillance, and Direction Finding*, Krieger Publishing Company, Malabar, FL, 1991.

9. Nielson, D.L., "Review of VHF transequatorial propagation," in *AGARD Conf. Proc., n.37, pt.2, Scatter Propagation of Radio Waves,* p.45/1-18, 1968.

10. Crackneil, R.G., Anderson, F., and Fimerelis, C., "The Euro-Asia to Africa VHF transequatorial circuit during solar cycle 21," *QST*, v.65, n.11, pp.31-36, v.65, n.12, pp.23-27, 1981.

11. McCue, C.G. and Fyfe, D.F., "Transequatorial propagation: Task Bridger introductory review," *Proc. IREE* (Aust.), v.26, pp.1-10, 1965.

12. Harrison, R.L., "Transequatorial propagation," *Amateur Radio* (Aust.). v.40, n.5-6, pp.3-6, 1972.

13. Villard, O.G., Stein, S., and Yeh, K.C., "Studies of transequatorial ionospheric propagation by the scatter-sounding method," *J. Geophys. Res.*, v.62, n.3, pp.399-412, 1957.

14. Uzunoglu, N.K., and Fimerelis, C., "A waveguide model for the evening type transequatorial VHF propagation: Comparison with experiment for the Euro-African sector," *Electromagnetics*, v.8, n.1, pp.1-13, 1988.

15. Gibson-Wilde, B.C., "Relation between the equatorial anomaly and transequatorial VHF radio propagation," *Radio Science*, v.4, n.9, pp.797-803, 1969.

16. Bowen, E.D., Fay, W.J., and Heritage, J.L., "VHF characteristics of the transequatorial ionosphere," *J. Geophys. Res.*, v.73, n.7, pp.2469-2476, 1968.

17. Nielson, D.L., "Long-range VHF propagation across the geomagnetic equator," Stanford Research Institute Report, Menlo Park CA, 1969.

18. Heron, M.L., and McNamara, L.F., "Transequatorial VHF propagation through equatorial plasma bubbles," *Radio Science*, v.14, n.5, pp.897-910, 1979.

19. Winkler, C., "Radio wave guidance at VHF through equatorial plasma bubbles," *J. Atm. Terr. Phys.*, v.43, n.4, pp.307-315, 1981.

20. Tsunoda, R. "Magnetic field-aligned characteristics of plasma bubbles in the night-time equatorial ionosphere," *J. Atm. Terr. Phys.*, v.42, pp.743-752, 1980.

21. Platt, I.G. and Dyson, P.L., "VHF transequatorial propagation via three dimensional waveguides," *J. Atm. Terr. Physics*, v. 51, n.11/12, pp.911-928, 1989.

22. Hatfield, V.E., and Smith, G., *AMBCOM User's Guide for Engineers*, SRI International, 1987.

23. Hatfield, V.E., and others, *AMBCOM User's Guide for Programmers: Part One--Description*, SRI International, 1987.

24. Hatfield, V.E., and others, *AMBCOM User's Guide for Programmers: Part Two--Listings*, SRI International, 1987.

25. Wilson, D.J., "A comparison of high-latitude ionosphere propagation predictions from AMBCOM with measured data," Master's thesis, Naval Postgraduate School, Monterey, CA, Mar. 1991.

26. Griffeths, J., *Radio Wave Propagation and Antennas*, Prentice-Hall International, Englewood Cliffs, NJ, 1987.

27. Carpenter, G., SRI International, in private telephone conversation, Jan. 1993.

BIBLIOGRAPHY

Aarons, J., "Construction of a model of equatorial scintillation intensity." *Radio Science*, v.20, n.3, pp.397-402, 1985.

Aarons, J., "Equatorial scintillations: A review," *IEEE Trans.* on Antennas and Propagation, v.AP-25, n.5, pp.729-736, 1977.

Aarons, J., "A survey of scintillation data and its relationship to satellite communications." Report AFCRL-70-0053, Air Force Cambridge Research Labs, Hanscom Field, MA, 1970.

Aarons, J., and Martin, E., "The effects of the August 1972 magnetic storms on ionospheric scintillations," *Radio Science*, v.10, n.5, pp.547-554, 1975.

Aarons, J., "Equatorial F-layer irregularity patches at anomaly latitudes," *J. Atm. Terr. Phys.*, v.47, p.875, 1985.

Aarons, J., and others, "Gigahertz scintillations associated with equatorial patches," *Radio Science*, v.18, n.3, pp.421-434, 1983.

Aarons, J., and Das Gupta, A., "Equatorial scintillations during the major magnetic storm of April 1981," *Radio Science*, v.19, n.3, pp.731-739, 1984.

Aarons, J., Whitney, H.E., and Allen, R.S., "Global morphology of ionospheric scintillations," Proc. IEEE, v.59, n.2, pp.159-172, 1971.

Abdu, M.A., and others, "Spread F plasma bubble vertical rise velocities determined from space ionosonde observations," Report INPE-2416, Instituto de Pesquisas Espaciais, Sao Jose Dos Campos (Brazil), 1982.

Abdu, M.A., Bittencourt, J.A., and Batista, I.S., "Magnetic declination control of the equatorial F region dynamo electric field development and spread F," *J. Geophys. Res.*, v.86, n.A13, pp.11443-11446, 1981.

Abdu, M.A., and others, "Equatorial ionospheric plasma bubble irregularity occurrence and zonal velocities under quiet and disturbed conditions, from polarimeter observations," *J. Geophys. Res.*, v.90, n.A10, pp.9921-9928, 1985.

Aksenov, V.I., and others, "Investigation of sporadic solar radio emission and parameters of the Earth's ionosphere by Intercosmos-Copernicus 500, VI. Morphological and spectral characteristics of electron density in the ionosphere." *Cosmic Research*, v.20, n.4, pp.383-391, 1982.

Anastassiadis, M., and Antoniadis, D., "Time delay measurements in the Athens (Greece)-Roma (Lesotho) VHF trans-equatorial propagation circuit," *J. Atm. Terr. Phys.*, v.34, pp.1215-1222, 1972.

Anastassiadis, M., and Stefanou, G., "Long range VHF transequatorial propagation for the European-African path: A review of time delay measurements," in AGARD-CP-173 on Radio Systems and the Ionosphere, p.9/1-22, 1976.

Anderson, D.A., and Bernhardt, P., "Modeling the effects of a H_2 gas release on the equatorial ionosphere," *J. Geophys. Res.*, v.83, p.4777, 1978.

Appleton, E.V., "Two anomalies in the ionosphere," *Nature*, v.157, p.691, 1946.

Appleton, E.V., "The anomalous equatorial belt in the F2 layer," *J. Atm. Terr. Phys.*, v.5, n.5/6, pp.348-351, 1954.

Argo, P.E., and Kelley, M.C., "Digital ionosonde observations during equatorial spread F," *J. Geophys. Res.*, v.91, n.A5, pp.5539-5555, 1986.

Argo, P.E., "Digital HF radar observations of equatorial spread-F," Report LA-UR-84-264, Los Alamos National Lab., NM, 1984.

Austin, B.A., "Ionospheric and geographical effects on the choice of tactical and point-to-point HF antenna systems," *Electronics Letters*, v. 21, n.23, pp.1107-1108, 1985.

Bain, W.F., "Unusual HF propagation modes as implied by observations of transmissions from the USSR and Red China," R-1152-0047A, presented at URSI Symposium (October 1964), University of Illinois, 1965.

Balan, N., and Rao, P.B., "Relationship between nighttime total electron content enhancements and VHF scintillations at the equator," *J. Geophys. Res.*, v.89, n.A10, pp.9009-9013, 1984.

Bandyopadhyay, P., and Chatterjee, S.K., "The blanketing sporadic-E near the magnetic equator: A review," *Indian J. of Radio & Space Physics*, v.16, n.1, pp.76-83, 1987.

Bandyopadhyay, P., and Aarons, J., "The equatorial F-layer irregularity extent as observed from Huancayo, Peru," *Radio Science*, v.5, n.6, pp.931-938, 1970.

Basler, R.P., and others. "Ionospheric distortion of HF signals," *Radio Science*, v.23, n.4. pp.569-579. 1988.

Basu, Sa., and others. "Gigahertz scintillations and spaced receiver drift measurements during Project Condor equatorial F region rocket campaign in Peru," *J. Geophys. Res.*, v.91, n.A5, pp.5526-5538, 1986.

Basu, Su., and others, "High resolution topside in-situ data of electron densities and VHF/GHz scintillations in the equatorial region," *J. Geophys. Res.*, v.88, n.A1, pp.403-415, 1983.

Basu, Su., and Basu, Sa., and Khan, B.K., "Model of equatorial scintillations from in-situ measurements," *Radio Science*, v.11, n.10, pp.821-832, 1976.

Basu, Sa., and others, "Scintillations associated with bottomside sinusoidal irregularities in the equatorial F region," *J. Geophys. Res.*, v.91, n.A1, pp.270-276, 1986.

Basu, Sa., and others, "250 MHz/GHz scintillation parameters in the equatorial, polar, and auroral environments," Report AFGL-TR-86-0070, Air Force Geophysics Lab, Hanscom AFB, MA, 1986.

Basu, Sa., and Whitney, H.E., "Temporal structure of intensity scintillations near the magnetic equator," *Radio Science*, v.18, n.2, pp.263-271, 1983.

Basu, S., MacKenzie, E., and Basu, S., "Ionospheric constraints on VHF/UHF communications links during solar maximum and minimum periods," *Radio Science*, v.23, n.3, pp.363-378, 1988.

Basu, Su, and Basu, Sa., "Equatorial scintillations: Advances since ISEA-6," *J. Atmos. Terr. Phys.*, v.47, nos. 8/10, pp.753-768, 1985.

Basu, Sa., and Basu, Su., "Equatorial scintillations - A review," *J. Atm. Terr. Phys.*, v.43, p.473, 1981.

Bhattacharyya, A., and Rastogi, R.G., "Multifrequency spectra of day-time ionospheric amplitude scintillations near the dip equator," *J. Atm. Terr. Phys.*, v.48, n.5, pp. 463-469, 1986.

Booker, H.G., "The role of acoustic gravity waves in the generation of spread-F and ionospheric scintillation," *J. Atm. Terr. Phys.*, v.41, n.5, pp.501-515, 1979.

Bowen, E.D., "Propagation characteristics of the equatorial ionosphere as measured between magnetically conjugate points at VHF," in *ESSA Conjugate Point Symp., v.2, session 3*, July, 1967.

Bowen, E.D., and others, "Transequatorial F-layer propagation study," Technical Report SRA-525, Smyth Research Associates, San Diego CA, AD-800339/4, Sep 1966.

Bowles, K.L., and Cohen, R.S., "A study of radio wave scattering from sporadic-E near the magnetic equator," *Ionospheric Sporadic-E* (Ed. Smith, E.K. and Matsushita, S.), Pergamon Press, 1962.

Bradley, P.A., Eccles, D., and King, J.W., "Some effects of the equatorial ionosphere on terrestrial HF radiocommunication," *Telecomm. J.*, v.39, n.12, pp.717-724, 1972.

Brayer, K., "Error patterns measured on transequatorial HF communication links," *IEEE Trans. Comm. Tech.*, v.COM-16, pp.215-221, 1968.

Calvert W., and others, "Equatorial spread-F motions," *Proc. Intern. Conf. Ionosphere*, 1962, pp. 316-322, Physical Society, London, 1963.

Calvert, W., "Equatorial spread F," NBS tech. Note 145, National Bureau of Standards, Boulder, CO, Aug 1, 1962.

Calvert, W., and Cohen, R., "The interpretation and synthesis of certain spread-F configurations appearing on equatorial ionograms," *J. Geophys. Research*, v.66, n.10, pp.3125-3140, 1961.

Campbell, Q., "A survey of VHF/UHF propagation modes. II.," *Radio Communication*, v.61, n.10, pp.772-776, 1985.

Carman, E.H., Gibson-Wilde, B.C., and Conway, J.R., "Anomalous VHF trans-equatorial ionospheric propagation recorded at Townsville," *Aust. J. Phys.*, v.16, n.1, pp.171-176, 1963.

Carman, E.H., Heeran, M.P., and Anastassiadis, M.A., "Investigation of a VHF transequatorial path between Europe and southern Africa," *J. Atm. Terr. Phys.*, v.35, pp.1213-1222, 1973.

Carman, E.H., Heeran, M.P., and Röttger, J., "Simultaneous observation of fading rates on two transequatorial HF radio paths," *Aust. J. Phys.*, v.27, n.5, pp.741-744, 1974.

Carman, E.H., and Heeran, M.P., "Trans-equatorial transmission at very high frequency," Technical Report RADC-TR-73-383, ADA054193, 1973.

Carman, E.H., Heeran, M.P., and Anastassiadis, M.A., "Trans-equatorial transmissions at very high frequency," Technical Report RADC-TR-71-143, AD728723, 1971.

CCIR, "Special problems of HF radiocommunication associated with the equatorial ionosphere," Report 343 in *Recommendations and Reports of the CCIR: v. II(Propagation)*, XIth Plenary Assembly held in Oslo, ITU, Geneva, 1967.

CCIR, "VHF propagation by regular layers, sporadic E, and other anomalous ionization," Report 259-6, in *Recommendations and Reports of the CCIR: Vol.6 (Propagation in Ionized Media)*, XVIth Plenary Assembly held in Dubrovnik, ITU, Geneva, 1986.

Chandra, H., and others, "Ionospheric scintillation observations from SHAR," *J. Atm. Terr. Phys.*, v.54, n.2, pp.167-172, 1992.

Chang, H., "The waveguide mode theory of whispering-gallery propagation in the F region of the ionosphere," *Radio Science*, v.6, n.4, pp.475-482, 1971.

Chang, H., "Whispering-gallery propagation in the E region of the ionosphere at HF and VHF," *Radio Science*, v.6, n.4, pp.465-473, 1971.

Clemesha, B.R., and Wright, R.W.H., "A survey of equatorial spread F, spread F and its effects on radiowave propagation," AGARDograph 95, pp.3-27, 1966.

Cohen, R., and McClure, J.P., "Transequatorial Propagation Implications of Equatorial Vertical Drift Measurements," in *AGARD Conf. Proc. n.37, pt.2, Scatter Propagation of Radio Waves*, p.49/1-9, 1968.

Cohen, R., "F-region scatter," in *AGARD Conf. Proc. n.37, pt.2, Scatter Propagation of Radio Waves*, p.51/1-12, 1968.

Cohen, R., and Bowles, K.L., "Association of plane-wave electron-density irregularities within the equatorial electrojet, *J. Geophys. Res.*, pp.2503-2525, 1963.

Cohen, R., and Bowles, K.L., "On the nature of equatorial spread F," *J. Geophys. Res.*, v.66, n.4, pp.1081-1106, 1961.

Cohen, R., and Bowles, K.L., "Ionospheric VHF scattering near the magnetic equator during the International Geophysical Year, *J. Res. Nat. Bur. Stand., Sect. D*, v.67, n.5, pp.459-479, 1963.

Cole, D.G., and McNamara, L.F., "Equatorial propagation and the occurrence of spread F," Proc. IREE Aust., v.36, n.3, pp.39-43, 1975.

Communication Laboratory, Stanford Research Institute, film on "Nuclear weapon effects on the ionosphere (F region disturbances)," prepared for U.S. Electronics Research and Development Laboratory, Fort Monmouth, NJ, Contract DA 36-039 SC-87197, DASA Subtask 07.104.

Cracknell, R.G., and Whiting, R.A., "Twenty-one years of TE, II. Transequatorial radiowave propagation," *Radio Communication*, v.56, n.8, pp.785-788, 1980.

Cracknell, R.G., and Whiting, R.A., "Twenty-one years of TE, I. Transequatorial radiowave propagation," *Radio Communication*, v.56, n.6-7, pp.626-634, 1980.

Cracknell, R.G., "Transequatorial propagation of VHF signals," *QST*, v.43, pp.11-17, 1959.

Crain, C.M., and Booker, H.G., "The effects of nuclear bursts in space on the propagation of high frequency radio waves between separated Earth terminals," *J. Geophys. Res.*, v.68, n.8, pp.2159-2166, 1963.

Crochet, M., and Broche, P., "Etude d'une propagation transequatoriale en dehors du grand cercle en periode d'occurrence de F diffus," in *AGARD Conf. Proc. n.37, pt.2, Scatter Propagation of Radio Waves*, p.47/1-9, 1968.

Dabas, R.S., Laksmi, D.R., and Reddy, B.M., "Effect of geomagnetic disturbances on the VHF nighttime scintillation activity at equatorial and low latitudes," *Radio Science*, v.24, n.4, pp.563-573, 1989.

Das Gupta, A., Lee, M.C., and Klobuchar, J.A., "VHF Faraday polarization fluctuations and strong L-band amplitude scintillations near Appleton anomaly crests," *Nature*, v.298, n.5872, pp.354-357, 1982.

Das Gupta, A.K., and Grossi, M.D., "Adaptive HF propagation path utilization," Report AFGL-TR-79-0236, Air Force Geophysics Lab, Hanscom AFB, MA, AD-A090023, 1980.

Das Gupta, A., Maitra, A., and Das, S.K., "Post-midnight equatorial scintillation activity in relation to geomagnetic disturbances," *J. Atm. Terr. Phys.*, v. 47, n.8-10, pp.911-916, 1985.

Das Gupta, A., and others, "VHF amplitude scintillations and associated electron content depletions as observed at Arequipa, Peru," *J. Atm. Terr. Phys.*, v.45, n.1, pp.15-26, 1983.

Das Gupta, A., Maitra, A., and Basu, Sa., "Occurrence of nighttime VHF scintillations near the equatorial anomaly crest in the Indian sector," *Radio Science*, v.16, n.6, pp.1455-1458, 1981.

Davies, K., and Rush, C.M., "Reflection of high-frequency radio waves in inhomogeneous ionospheric layers," *Radio Science*, v.20, n.3, pp.303-309, 1985.

Davies, K., and Rush, C.M., "Reflection of high-frequency radio waves in inhomogeneous ionospheric layers," *Radio Science*, v.20, n.3, pp.303-309, 1985.

Davies, K., and Barghausen, A.F., "The effect of spread F on the propagation of radiowaves near the magnetic equator," in *Spread F and its Effect upon Radiowave Propagation and Communication*, P. Newman(editor), NATO-AGARDograph 95, Technivision, Maidenhead, England, 1966.

Davies, K., *Ionospheric Radio Propagation*, National Bureau of Standards Monograph 80, 1 April 1965.

Davies, K., and Barghausen, A.F., "The effect of spread F on the propagation of radio waves near the equator," in *Ninth Meeting of Ionospheric Research Committee*, AGARD, Copenhagen, Denmark, 1964.

Davies K., and Chang, N., "Radio-doppler observations of the ionosphere near the magnetic equator," in *Scatter Propagation of Radio Waves*, AGARD Conf. Proc., 37, 52-1-52-6, 1968.

De Medeiros, R.T., Abdu, M.A., and Kanto, I.J., "A comparative study of VHF scintillation and spread F events over Natal and Fortaleza in Brazil," *J. Geophys. Res.*, v.88, n.A8, pp.6253-6258, 1983.

Depaula, E.R., and Abdu, M.A., "Behavior of the ionospheric F region in low latitudes and in the equatorial region of Brazil during strong magnetic storms in the 1978 to 1983 period," Report INPE-3231-PRE/581, Instituto de Pesquisas Espaciais, Sao Jose Dos Campos (Brazil), 1984.

Doeppner, T.W., Hagn, G.H., and Sturgill, L.G., "Electromagnetic propagation in a tropical environment," *J. Defense Research, Series B, Tactical Warfare*, v.4B, n.4, pp.353-404, 1973.

Dueño, B., "Peculiarities and seasonal variations of transequatorial backscatter echoes as observed at Mayagüez, Puerto Rico," *J. Geophys. Res.*, v.65, pp.1691-1698, 1960.

Farley, D.T., "Theory of equatorial electrojet plasma waves: New developments and current status," *J. Atm. Terr. Phys.*, 47, p. 729, 1985.

Fejer, B.G., and others, "Vertical structure of the VHF backscattering region in the equatorial electrojet and the gradient drift instability," *J. Geophys. Res.*, v.80, n.10, pp.1313-1323, 1975.

Fejer, B.G., Kudeki, E., and Farley, D.T., "Equatorial F region zonal plasma drifts," *J. Geophys. Res.*, v.90, n.A12, pp.12249-12255, 1985.

Ferguson, J.A., and Booker, H.G., "A scattering theory of VHF transequatorial propagation," *J. Atm. Terr. Phys.*, v.45, n.8-9, pp.641-657, 1983.

Ferguson, J.A., "Application of a scattering theory of VHF transequatorial propagation," *J. Atm. Terr. Phys.*, v.46, n.8, pp.643-661, 1984.

Ferrell. O.P., "Enhanced trans-equatorial propagation following geomagnetic storms," *Nature*, v.167, p.811, 1951.

Fimerelis, C., and Uzunoglu, N.K., "Transequatorial propagation on VHF and low UHF bands during the peak of solar cycle 21 for the Euro-African sector," in *IEEE 1981 International Symposium Digest, Antennas and Propagation,* v.2, pp.379-382, 1981.

Franke, S.J., and Liu, C.H., "Observations and modeling of multi-frequency VHF and GHz scintillations in the equatorial region," *J. Geophys. Res.*, v.88, n.A9, pp.7075-7085, 1983.

Franke, S.J., and Liu, C.H., "Modeling of equatorial multifrequency scintillation," *Radio Science,* v.20, n.3, pp.403-415, 1985.

Freeman, R.L., *Telecommunication Transmission Handbook*, 3rd ed., John Wiley & Sons, Inc., 1991.

Fulks, G.J., "ISIS topside sounder data gathered on Kwajalein atoll during the summers of 1977 and 1978," Report MRC-R-548, Mission Research Corp, Santa Barbara, CA, ADA091845, 1980.

Gerson, N.C., "Ray tracing over a trans-equatorial path," in *AGARD Conf. Proc. n.37, pt.2, Scatter Propagation of Radio Waves*," p.48/1-23, 1968.

Gibson-Wilde, B.C., "The equatorial anomaly in the Australasian zone during sunspot minimum," *J. Atm. Terr. Phys.*, v.29, pp.1269-1275, 1967.

Gibson-Wilde, B.C., and Carman, E.H., "Further studies of long-range transequatorial VHF radio signals at Townsville," *J. Atm. Terr. Phys.*, v.26, pp.1231-1237, 1964.

Goodman, J.M. and Aarons, Jules, "Ionospheric effects on modern electronic systems," *Proc. IEEE*, v.78, n.3, pp.512-526, 1990.

Goodman, J.M., "Effect of the ionosphere on radiowave systems," *Conf. Proc. of Ionospheric Effects Symposium (IES '81)*, AD-A118236/9, Apr 1981.

Goodman, J.M., "Effect of the ionosphere on space and terrestrial systems," Ionospheric Effects Symposium, Arlington, VA, AD-A100160/1, Jan 1978.

Gurevich, A.G., and Tsedilina, E.E., *Long Distance Propagation of HF Radio Waves*, Springer, Heidelberg, Federal Republic of Germany, 1985.

Hagn, G.H., "Absorption of ionospherically propagated HF radio waves under conditions where the quasi-transverse (Qt) approximation is valid," Report STR-9, Stanford Research Institute, Menlo Park, CA, AD-480588/3, 1964.

Hagn, G.H., and Posey, K.A., "Survey of literature pertaining to the equatorial ionosphere and tropical communications," Special Report on SRI Proj. 4240, Stanford Research Institute, Menlo Park CA, AD 486800, 1966.

Hagn, G.H., and Barker, G.E., "Research-engineering and support for tropical communications," Final Report, Contract DA-36--039 AMC-00040(E), SRI Project 4240, Stanford Research Institute, Menlo Park CA, AD-889169, 1970.

Hagn, G.H., "Orientation of linearly polarized HF antennas for short-path communication via the ionosphere near the geomagnetic equator," Report on SRI Project 4240, Stanford Research Institute, Menlo Park CA, AD 480592, 1964.

Haldoupis, C., "A review on radio studies of auroral E-region ionospheric irregularities," *Annales Geophysicae: Atmospheres, Hydrospheres, and Space Sciences*, v.7, n.3, pp.239-258, 1989.

Hanson, W.B., and Moffett, R.J., "Ionization transport effects in the equatorial F region," *J. Geophys. Res.* , v.71, pp. 5559-5568, 1966.

Heritage, J.L., and Bowen, E.D., "Transequatorial 'F' layer study," Technical Report SRA-503, Smyth Research Associates, San Diego CA, AD-633428, Apr 1966.

Heeran, M.P., and Carman, E.H., "Transequatorial VHF transmission and solar-related phenomena," *Aust. J. Phys.*, v.26, n.6, pp.797-804, 1973.

Herman, J.R., "Spread F and ionospheric F region irregularities," *Rev. Geophys. Space Phys.*, v.4, pp.255-299, 1966.

Heron, M.L., "Recent progress in transequatorial propagation-Review," *J. Atm. Terr. Phys.*, v.43, n.5-6, pp.597-606, 1981.

Heron, M.L., "On transequatorial VHF propagation paths," *J. Atm. Terr. Phys.*, v.43, n.8, pp.867-871, 1981.

Heron, M.L., "Transequatorial propagation through equatorial plasma bubbles-Discrete events," *Radio Science*, v.15, n.4, pp.829-835, 1980.

Hortenbach, K.J., and Rogler, F., "On the propagation of short waves over long distances: Predictions and observations," *Telecomm. J.*, v.46, pp.320-329, 1979.

Huang, Y.N., "Ionospheric electron content depletion associated with amplitude scintillation at the equatorial anomaly crest region," *J. Geophys. Res.*, v.90, n.A4, pp.4333-4339, 1985.

Jayachandran, B., and others, "HF doppler observations of vertical plasma drifts in the evening F region at the equator," *J. Geophys. Res.*, v.92, n.A10, p.11253-11256, 1987.

Jursa, A.S. (Scientific Editor), *Handbook of Geophysics and the Space Environment*, Air Force Geophysics Laboratory, Air Force Systems Command, U.S. Air Force, NTIS, Springfield, VA, 1985.

Karpachev, A.T., "Characteristics of the global longitude effect in the nighttime equatorial anomaly," *Geomagnetism and Aeronomy*, v.28, n.1, pp.35-38, 1988.

Kelleher, R.F., and Röttger, J., "Equatorial spread-F irregularities observed at Nairobi and on the transequatorial path Lindau-Tsumeb," *J. Atm. Terr. Phys.*, v.35, pp.1207-1211, 1973.

King, G.A.M., "Spread-F on ionograms," *J. Atm. Terr. Phys.*, v.32, pp.209-231, 1970.

Klobuchar, J.A., and Lee, M.C., "Periodic amplitude variations as precursors of plumes of equatorial ionospheric irregularities," *J. Atm. Terr. Phys.*, v.51, n.9-10, pp.733-738, 1989.

Klobuchar, J.A., Anderson, D.N., and Doherty, P.H., "Model studies of the latitudinal extent of the equatorial anomaly during equinoctial conditions," *Radio Science*, v.26, n.4, pp.1025-1047, 1991.

Knecht, D.J. and Shuman B.M., "The geomagnetic field," in *Handbook of Physics and the Space Environment*, edited by A.S. Jursa, AFGL, NTIS, Springfield, VA, 1985.

Koparkar, P.V., Rastogi, R.G., and Sastri, J.H., "Daytime equatorial VHF radiowave scintillations and sporadic-E layer," *Indian J. of Radio & Space Physics*, v.18, n.4, pp.121-124, 1989.

Koparkar, P., "Radio scintillations near the F-region anomaly crest," *Indian J. of Radio & Space Physics*, v.16, n.5, p.357-359, 1987.

Koparkar, P.V., and Rastogi, R.G., "Geomagnetic disturbance effect on equatorial radio wave scintillations," *Current Science*, v.55, n.3, pp.126-128, 1986.

Koparker, P.V., Pathan, B.M., and Rastogi, R.G., "East-west movement of ionospheric irregularities causing equatorial radio wave scintillations," *Indian J. Radio & Space Physics*, v.20, n.5, pp.333-337, 1991.

Koster, J.R. and Wright, R.W., "Scintillation, spread F, and transequatorial scatter," *J. Geophys. Research*, v.65, pp.2303-2306, 1960.

Koster, J.R., "Equatorial scintillation," *Planetary and Space Science*, v.20, pp.1999-2014, 1972.

Kudeki, E., and others, "The Condor equatorial electrojet campaign: Radar results," *J. Geophys. Res.*, v.92, n.A12, pp.13561-13577, 1987.

Kuriki, I., and others, "Investigations of the transequatorial propagation mode in the VHF Band," *J. Radio Res. Lab.* (Japan), v.15, n.80-81, pp.199-217, 1968.

Kuriki, I., and others, "Propagational mode deducted from signal strengths in the VHF band on the trans-equatorial path," *J. Radio Res. Labs* (Japan), v.19, n.100, pp.175-195, 1972.

Lakshmi, D.R., Reddy, B.M., and Shastri, S., "A prediction model for equatorial and low latitude HF communication parameters during magnetic disturbances," *Indian Jour. Radio & Space Physics*, v.12, n.4, pp.118-123, 1983.

Lane, G., and Richardson, A., "Super modes and IONCAP," paper contained in HF-MAP Newsletter(Winter Edition), Naval Research Laboratory, Washington D.C., 1990.

Laxmi, V.N., and Tripathi, V.K., "Radio wave heating and equatorial spread-F," *J. Atm. Terr. Phys.*, v.49, n.11-12, pp.1071-1074, 1987.

Lee, M.C., and others, "Depolarization of VHF geostationary satellite signals near the equatorial anomaly crests," *Radio Science*, v.17, n.2, pp.399-409, 1982.

Lee, M.C., "Faraday polarization fluctuations of transionospheric propagation," *J. Geophys. Res.*, v.87, n.A2, pp.751-755, 1982.

Lomax, J.B., "Spread-F in the Pacific," in *Spread F and its Effects upon Radiowave Propagation and Communication*, P. Newman(editor), NATO-AGARDograph 95, Technivision, Maidenhead, England, 1966.

Lomax, J.B., and Kitts, H.L., "HF communications experiment description, Operation Dominic, Fish Bowl series," Interim Report 1, Contract DA 06-038 SC-87197, SRI Project 3670, Stanford Research Institute, Menlo Park, CA, Jul 1962.

Lomax, J.B., Nielson, D.L., and Nelson, R.A., "Contour maps of critical frequency illustrating effects on the ionosphere of high-altitude nuclear tests (U)," DASA 1657, May 1965.

Lomax, J.B., and Nielson, D.L., "Observation of acoustic-gravity wave effects showing geomagnetic field dependence," *J. Atm. Terr. Phys.*, v.330, pp.1033-1050, 1968.

Lunnen, R.J., and others, "Detection of radiation from a heated and modulated equatorial electrojet current system," *Nature*, v.311, n.5982, pp.134-135, 1984.

Mathew, B., and others, "Comparative study of scintillations at the magnetic equator and at the crest region of the equatorial anomaly in the Indian zone," *Proc. of the Indian Academy of Sciences, Earth and Planetary Sciences*, v.100, n.4, pp.331-340, 1991.

Mathew, B., Iyer, K.N., and Pathan, B.M., "Patchy occurrence of VHF scintillations at tropical latitudes," *J. Atm. Terr. Phys.*, v.54, n.7-8, pp.963-968, 1992.

Matuura, N., Koizumi, T., and Yamaoka, M., "Ionospheric storm during the event of August 1972," *Report of Ionosphere and Space Research in Japan*, v.27, n.4, pp.179-180, 1973.

McClure, J.P., "Electron density studies at Jicamarca," in De Mendonça, F. (Ed.). *Equatorial Aeronomy*, Brazil Space Commission, Brazilia, Brazil, p.170, 1965.

McCue, C.G., "Proposal of a new theory of transequatorial V.H.F. radio wave propagation anomalies," Technical Report WRE-TN-CPD/T/-121, Australian Defense Scientific Service, Weapons Research Establishment, Salisbury (Australia), Apr 1965.

McNamara, L.F., "Ionospheric predictions on transequatorial circuits," *Proc. IREE (Aust.)*, v. 35, n. 5, pp.117-126, 1974.

McNamara, L.F., *The Ionosphere: Communications, Surveillance, and Direction Finding*. Krieger Publishing Company, 1991.

McNamara, L.F., "Evening-type transequatorial propagation on Japan-Australia circuits." *Aust. J. Physics*, v.26, pp.521-543, 1973.

Moision, W.K., Hildebrand, V.E., and Rose, R.B., "Analysis of predicted maximum usable frequency and maximum observed frequency over a Guam-to-Australia transequatorial path," Technical Report N. NWC-TP-4906, Naval Weapons Center, China Lake CA, AD870967/7, May 1970.

Möller, H.G., "Sweep frequency propagation on a 8000 Km transequatorial north south path," in AGARD-CP-173 on Radio Systems and the Ionosphere, p.13/1-7, January 1976.

Moraitis, G., Vassilaras, J., and Anastassiadis, M., "Movement of the reflecting layer in the trans-equatorial propagation path Athens(Greece)-Roma(Lesotho)," *J. Atm. Terr. Phys.*, v.35, n.12, pp.2283-2288, 1973.

Morse, F.A., and others, "EQUION, an equatorial ionospheric irregularity experiment," *J. Geophys. Res.*, v.82, n.4, pp.578-592, 1977.

Muldrew, D.B., "Radio propagation along magnetic field-aligned sheets of ionization observed by the Alouette topside sounder," *J. Geophys. Research*, v.68, n.19, pp.5355-5370, Oct 1963.

Muldrew, D.B., "Nonvertical propagation and delayed-echo generation observed by the Topside sounders," *IEEE Proc.*, v.57, n.6, pp.1097-1107, Jun 1969.

Muralikrishna, P., and Abdu, M.A., "In-situ measurement of ionospheric plasma density by two different techniques - a comparison," *J. Atm. Terr. Phys.*, v.53, n.8, pp.787-793, 1991.

Nair, R.B., and others, "Spectra of the AC electric fields in the post-sunset F-region at the magnetic equator," *Planetary and Space Science*, v.40, n.5, pp.655-662, 1992.

Namboothiri, S.P., Balan, N., and Rao, P.B., "Vertical plasma drifts in the F region at the magnetic equator," *J. Geophys. Res.*, v.94, n.A9, pp.12055-12060, 1989.

Namboothiri, S.P., and others, "Vertical Plasma Drifts in the Post-Sunset F-Region at the Magnetic Equator," *J. Atm. Terr. Phys.*, v.50, n.12, pp.1087-1091, 1988.

Nelson, O.R., "Time and latitudinal distribution of the ionospheric irregularities in Brazil, through the VHF-scintillation and ionogram data analysis," Report INPE-3179, Instituto de Pesquisas Espaciais, Sao Jose Dos Campos (Brazil), 1984.

Newman, P., Jones, B., and McCabe, L., "F-region irregularities after high altitude detonation of July 9, 1962," in *Spread F and its Effects upon Radiowave Propagation and Communication*, P. Newman(editor), NATO-AGARDograph 95, Technivision, Maidenhead, England, 1966.

Nielson, D.L., and Crochet, M., "Ionospheric propagation of HF and VHF radio waves across the geomagnetic equator," *Rev. Geophys. and Space Phys.*, v.12, n.4, pp.688-702, 1974.

Nielson, D., "Oblique sounding of a trans-equatorial path," in *Spread F and its Effects upon Radiowave Propagation and Communication*, P. Newman(editor), NATO-AGARDograph 95, Technivision, Maidenhead, England, 1966.

Nielson, D.L., "The importance of horizontal F-region drifts to transequatorial VHF propagation," in *AGARD Conf. Proc. n.37, pt.2, Scatter Propagation of Radio Waves*, p.46/1-6, 1968.

Obayashi, Tatsuzo, "A possibility of the long distance HF propagation along the exospheric field-aligned ionizations," *Report of Ionosphere and Space Research, Japan*, v.13, n.3, Sep 1959.

Oyinloye, J.O., "Equatorial HF radio wave absorption measurements and the IRI," *J. Atm. Terr. Phys.*, v.50, n.6, pp.519-522, 1988.

Pathan, B.M., Rastogi, R.G., and Rao, D.R.K., "On the width of complexities of the equatorial nighttime radio wave scintillation belt in the Indian region," *J. Geomagnetism and Geoelectricity*, v.44, n.2, pp.129-142, 1992.

Piggott, W.R., "The calculation of the median sky-wave field strength in tropical regions," DSIR Radio Research Special Report 23, Her Majesty's Stationary Office, London, 1959.

Platt, I.G., and Dyson, P.L., "MF and HF ducting within equatorial bubbles," *J. Atm. Terr. Phys.*, v.51, n.9-10, pp.775-780, 1989.

Prabhakaran Nayar, S.R., and others, "HF doppler spectrum under spread F and nonspread F conditions at magnetic equator," in *Seventh International Conference on Antennas and Propagation ICAP 91*, (Conf. Publ. No.333). v.2, pp.902-905, 1991.

Prakash, S., and Pal, S., "Studies of electron density irregularities during strong spread-F," *Advances in Space Research*, v.5, n.7, pp.39-42, 1985.

Prakash, S., and Pal, S., "Electric fields and electron density irregularities in the equatorial electrojet," *J. Atm. Terr. Phys.*, v.47, n.8-10, pp.853-866, 1985.

Rangaswamy, S. and Kapasi, K.B., "A study of equatorial spread F," *J. Atm. Terr. Phys.*, v.25, pp.721-731, 1963.

Rastogi, R.G., and Mullen, J., "Intense daytime radio wave scintillations and sporadic E layer near the dip equator," *J. Geophys. Res.*, v.86, n.A1, pp.195-198, 1981.

Rastogi, R.G., "Equatorial E region electric field changes associated with a geomagnetic storm sudden commencement," *J. Geophys. Res.*, v.81, n.4. pp.687-689, 1976.

Rastogi, R.G., "Tropical spread-F," *Indian Jour. Radio & Space Physics*, v.12, n.4, pp.104-113, 1983.

Rastogi, R.G., Rangarajan, G.K., and Somayajulu, V.V., "Complexities of counter equatorial electrojet currents," *Indian Journal of Radio & Space Physics*, v.21, n.2, pp.89-96, 1992.

Rastogi, R.G., and others, "Daytime VHF radio wave scintillations at equatorial latitudes," *J. Geomagnetism and Geoelectricity*, v.43, n.7, pp.549-561, 1991.

Rastogi, R.G., "Onset of equatorial radio scintillations on different frequencies," *Indian Jour. Radio & Space Physics*, v.12, n.5, pp.150-155, 1983.

Rastogi, R.G., Koparker, P.V., and Pathan, B.M., "Nighttime radio wave scintillation at equatorial stations in Indian and American zones," *J. Geomagnetism and Geoelectricity*, v.42, n.1, pp.1-10, 1990.

Rastogi, R.G., "Equatorial VHF backscattering and scintillations related to ionospheric spread-F," *Indian J. of Radio & Space Physics*, v.15, n.2, pp.37-45, 1986.

Rastogi, R.G., and Aarons, J., "Nighttime ionospheric radio scintillations and vertical drifts at the magnetic equator," *J. Atm. Terr. Phys.*, v.42, pp.583-591, 1980.

Rastogi, R.G., "On the occurrence of equatorial spread-F in the evening hours," *J. Atm. Terr. Phys.*, v.48, n.8, pp.687-693, 1986.

Rastogi, R.G., Alex, S., and Koparkar, P.V., "Equatorial spread F and ionospheric electron content at low latitudes," *J. Geomagnetism and Geoelectricity*, v.41, n.9, pp.753-767, 1989.

Rastogi, R.G., Mullen, J.P., and MacKenzie, E., "Effect of geomagnetic activity on equatorial radio VHF scintillations and spread F," *J. Geophys. Res.*, v.86, n.A5, pp.3661-3664, 1981.

Rastogi, R.G., "Post-sunrise equatorial spread-F and radio scintillations," *Indian Jour. Radio & Space Physics*, v.12, n.6 pp.184-189, 1983.

Rastogi, R.G., Patil, A., and Alex, S., "Post-sunset uplifting of the equatorial F layer of the ionosphere and vertical plasma drift velocities," *J. Geomagnetism and Geoelectricity*, v.43, n.7, pp.607-611, 1991.

Rastogi, R.G., and Koparker, P.V., "Ionospheric electron content over the magnetic equator during spread F conditions," *J. Geophys. Res.*, v.95, n.A1, pp.247-250, 1990.

Rastogi, R.G., "Early phase of equatorial spread-F seen by HF ionosonde and VHF backscatter radar," *Indian J. Radio & Space Physics*, v.10, n.4, pp.148-152, 1981.

Rastogi, R.G., "Equatorial electrojet and radio scintillations," *J. Atm. Terr. Phys.*, v.45, n.10, pp.719-728, 1983.

Rastogi, R.G., "Study of equatorial ionospheric F-region irregularities by reflection, backscatter and transmission of radio waves," *Indian Jour. Radio & Space Physics*, v.13, n.3, pp.84-93, 1984.

Rastogi, R.G., Mullen, J.P., and MacKenzie, E., "Effect of geomagnetic activity on equatorial radio VHF scintillations and spread F," *J. Geophys. Res.*, v.86, n.A5, pp.3661-3664, 1981.

Ravichandran, V.C., and Mukunda Rao, M., "Transequatorial propagation of TV Signals via sporadic-E," *J. Inst. of Electronics and Telecommunication Engineers*, v.38, n.1, pp.52-56, 1992.

Reinisch, B.W., "New techniques in ground-based ionospheric sounding and studies," *Radio Science*, v.21, n.3, pp.331-341, 1986.

Röttger, J., "Influence of spread-F on HF radio systems," in *AGARD Conf. Proc. n.173 on Radio Systems and the Ionosphere*, p.26/1-19, 1976.

Röttger, J. "Phenomenology of transequatorial radio propagation under spread-F conditions," *AGARD Conf. Proc. n.263 on Special Topics in HF Propagation*, p.24/1-24, 1979.

Röttger, J., "The phenomenology of transequatorial radio propagation under spread-F conditions," *AGARD Conf. Proc. n.263 on Special Topics in HF Propagation*, p.24/1-9, 1979.

Röttger, J., "Long-distance transequatorial propagation in the 144 MHz amateur radio band," *Telecomm. J.*, v.46, n.2, pp.120-121, 1979.

Röttger, J., "Wavelike structures of large-scale equatorial spread-F irregularities," *J. Atm. Terr. Phys.*, v.35, n.6, p.1195-1206, 1973.

Röttger, J. "Great-circle deviation of short wave signals resulting from scattering and reflection by ionospheric irregularities. Effect on radio navigation and communication, exemplified by transequatorial short wave propagation, Report BMVG-FBWT-75-9, Max-Planck-Institut fuer Aeronomie, Lindau Uber Northeim, 1975.

Röttger, J., "Some properties of large-scale equatorial spread-F irregularities interpreted by influences of atmospheric gravity waves," *Z. Geophys.*, v.39, p.799, 1973.

Royrvik, O., "Drift and aspect sensitivity of scattering irregularities in the upper equatorial E region," *J. Geophys. Res.*, v.87, n.A10, pp.8338-8342, 1982.

Saha, S.K., Pathan, B.M., and Rao, D.R.K., "VHF radio wave oscillations at Bangalore, a station near the fringe of equatorial electrojet," *National Acad. Science Letters*, v.12, n.6, pp.201-204, 1989.

Sastri, J.H., and others, "Origin of short-period(30-300 s) doppler frequency fluctuations of lower F region reflections in the equatorial electrojet region," *Radio Science*, v.26, n.6, pp.1403-1413, 1991.

Sastri, J.H., Ramesh, K.B., and Rao, J.V.S.V., "Doppler frequency fluctuations of lower thermospheric reflections in the equatorial electrojet region," *J. Atm. Terr. Phys.*, v.53, n.6-7, pp.567-576, 1991.

Sen, A.K., and Trehan, S.K., "Transequatorial propagation of HF Signal in relation to equatorial anomaly," *Indian J. Radio & Space Phys.*, v.3, n.3, pp.253-254, 1974.

Sen, A.K., and Trehan, S.K., "Propagation characteristics of HF signal over a transequatorial path," *Indian J. Radio & Space Phys.*, v.4, n.4, p.334, 1975.

Smith, E.K., and Finney, J.W., "Peculiarities of the ionosphere in the Far East: A report on IGY observation of sporadic E and F-region scatter," *J. Geophys. Res.*, v.65, pp.885-892, 1960.

Somayajulu, V.V., Reddy, C.A., and Viswanathan, K.S., "Simultaneous electric field changes in the equatorial electrojet in phase with polar cusp latitude changes during a magnetic storm," *Geophys. Res. Letters*, v.12, n.7, pp.473-475, 1985.

Southworth, M.P., "Night-time equatorial propagation at 50 MHz: First results from an IGY amateur observing program," *J. Geophys. Research*, v.65, pp.601-607, 1960.

Srirama Rao, M., Ramesh, K.S., and Niranjan, K., "Nocturnal F-region vertical drifts over Waltair," *Indian Jour. Radio & Space Physics*, v.20, n.5, pp.327-332, 1991.

Stein, S., "The role of ionospheric layer tilts in long-range high frequency radio propagation," *J. Geophys. Res.*, v.63, n.1, pp.217-241, 1958.

Sweeney, L.E., "Suggestions for future research in HF ionospheric modification," *Radio Science*, v.9, pp.1089-1090, 1974.

Tao, K., and others, "Experimental results of VHF trans-equatorial propagation," *J. Radio Res. Lab. Jap.*, v.17, n.89, pp.83-101, 1970.

Towle, D.M., "VHF and UHF radar observation of equatorial F region ionospheric irregularities and background densities," *Radio Science*, v.15, n.1, pp.71-86, 1980.

Tsunoda, R.T., "Time evolution and dynamics of equatorial backscatter plumes, I. Growth phase," *J. Geophys. Res.*, v.86, n.A1, pp.139-149, 1981.

Valley, S.L., (editor), *Handbook of Geophysics and Space Environment*, Air Force Cambridge Research Laboratories, Office of Aerospace Research, USAF, Hanscom AFB, Bedford MA, 1965.

Van Zandt, T.E., Loftees, B.T., and Calvert, W., "Explorer XX observations of conjugate ducts," *Proc. of Second International Symposium on Equatorial Aeronomy*, pp. 325-327, Brazilian Space Commission, São José dos Campos, São Paulo, Brazil, Nov 1965.

Viswanathan, K.S., Namboothiri, S.P., and Rao, P.B., "VHF and HF radar measurements of E and F region plasma drifts at the magnetic equator," *J. Geophys. Res.*, v.97, n.A3, pp.3011-3017, 1992.

Washburn, C.L., and others, "Trans-equatorial F-layer propagation study," ITT Report, Project 4505, Task 450504, Contract AF 30(602)-2506, 14 Jun 1963.

Wernik, A.W., and others, "Nighttime VHF and GHz scintillations in the East-Asian sector of the equatorial anomaly," *Geophys. Res. Letters*, v.10, n.2, pp.155-158. 1983.

Whale, H.A., *Effects of Ionospheric Scattering on Very Long Distance Radio Communications*, Plenum Press, NY, 1969.

Whitehead, J.D., "Recent work on mid-latitude and equatorial sporadic-E," *J. Atm. Terr. Physics*, v.51, n.5, pp.401-424, 1989.

Whitney, H.E., and Basu, Sa., "The effect of ionospheric scintillation on VHF/UHF satellite communications," *Radio Science*, v.12, n.1, pp.123-133, 1977.

Wright, R.W., and Skinner, N.J., "Equatorial spread F," *J. Atm. Terr. Phys.*, v.15, p.121, 1959.

Yamaoka, M., Tanohata, K., and Tsuchiya, K., "Solar-terrestrial disturbances of August 1972, XI. Anomalous propagation of VHF waves in the trans-equatorial paths," *J. Radio Res. Labs* (Japan), v.21, n.106, pp.405-422, 1974.

Yeh, K.C., and Villard, O.G., "A new type of fading observable on high-frequency radio transmission propagated over paths crossing the magnetic equator," *Proc. IRE*, v.46, p.1968-1970, 1958.

Yeh, K.C., and Villard, O.G., "Fading and attenuation of high frequency radio waves propagated over long paths crossing the auroral, temperate, and equatorial Zones," *J. Atm. Terr. Phys.*, v.23, pp.137-154, 1961.

Yeh, K.C., Soicher, H., and Liu, C.H., "Observations of equatorial ionospheric bubbles by the radio propagation method," *J. Geophys. Res.*, v.84, n.A11, pp.6589-6594, 1979.

Yinn-nien Huang, Kang Cheng, and Sen-wen Chen, "On the equatorial anomaly of the ionospheric total electron content near the northern anomaly crest region," *J. Geophys. Res.*, v.94, n.A10, pp.13515-13525, 1989.

Yinn-nien Huang, Kang Cheng, and Sen-wen Chen, "Daily observations of the development of the ionospheric equatorial anomaly by means of differential doppler shift method," *Radio Science*, v.22, n.3, pp.433-438, 1987.

INITIAL DISTRIBUTION LIST

		No. Copies
1.	Defense Technical Information Center Cameron Station Alexandria VA 22304-6145	2
2.	Library, Code 52 Naval Postgraduate School Monterey CA 93943-5002	2
3.	Chairman, Code EC Department of Electrical and Computer Engineering Naval Postgraduate School Monterey, CA 93943	1
4.	Professor R. W. Adler, Code EC/Ab Department of Electrical and Computer Engineering Naval Postgraduate School Monterey, CA 93943	5
5.	Professor W. R. Vincent, Code EC/Ab Department of Electrical and Computer Engineering Naval Postgraduate School Monterey, CA 93943	1
6.	Bob R. Rose NRaD, Code 542 Naval Command, Control and Ocean Surveillance Center 271 Catalina Blvd San Diego, CA 92152-5000	1
7.	Naval Security Group Command Code GX (CDR. G.K. Lott) 3801 Nebraska Ave NW Washington, DC 20393-5220	1

8. LT John W. McKinstry 1
Naval Research Laboratory
Code 9110
4555 Overlook Ave.
Washington, DC, S.W. 20345

8. LT John W. McKinstry
Naval Research Laboratory
Code 9110
4555 Overlook Ave.
Washington, DC, S.W. 20365